CORTEX

Research and Innovation Action (RIA)

This project has received funding from the European Union's Horizon 2020 research and innovation programme under grant agreement No 754316.

Start date : 2017-09-01 Duration : 48 Months
http://cortex-h2020.eu

Experimental report of the 2nd campaign at AKR-2 and CROCUS

Authors : Dr. Vincent LAMIRAND (EPFL), Sebastian HUEBNER (TUD), Alexander KNOSPE (TUD), Dr. Klemen AMBROZIC (EPFL), Dr. Oskari PAKARI (EPFL), Fanny VITULLO (EPFL), Dr. Carsten LANGE (TUD), Dr. Adolfo RAIS (EPFL)

CORTEX - Contract Number: 754316

Project officer: Marco Carbini

Document title	Experimental report of the 2nd campaign at AKR-2 and CROCUS
Author(s)	Dr. Vincent LAMIRAND, Sebastian HUEBNER (TUD), Alexander KNOSPE (TUD), Dr. Klemen AMBROZIC (EPFL), Dr. Oskari PAKARI (EPFL), Fanny VITULLO (EPFL), Dr. Carsten LANGE (TUD), Dr. Adolfo RAIS (EPFL)
Number of pages	33
Document type	Deliverable
Work Package	WP02
Document number	D2.2
Issued by	EPFL
Date of completion	2021-03-11 09:50:42
Dissemination level	Public

Summary

In the framework of the CORTEX project, the work package 2 targets the generation of high quality neutron noise experimental data for the subsequent validation of computer methods and models developed in work package 1. The AKR-2 reactor at TUD, and the CROCUS reactor at EPFL, are the experimental facilities where noise-specific experimental data are being generated. This report documents the experimental setup and measurements for each perturbation type and facility of the second campaigns. The raw time series will be distributed to the members of the consortium. The associated experimental results will be documented in separate internal reports and distributed to the members of the consortium.

Approval

Date	By
2021-03-11 10:07:18	Mr. Mathieu HURSIN (EPFL)
2021-03-11 10:08:31	Pr. Christophe DEMAZIERE (Chalmers)

Table of contents

Index of Tables

Index of Figures

Abbreviations

AC	Alternating Current
AVS	Absorber of Variable Strength
BB	Beagle-Bone
BNC	Bayonet Neill–Concelman connector
CIC	Compensated Ionization Chamber
COLIBRI	CROCUS Oscillator for Lateral Increase Between u-metal Rods and Inner zone
DAQ	Data acquisition system
DC	Direct Current
ECCP	Electronic Collaborative Content Platform
EPFL	Ecole Polytechnique Fédérale de Lausanne
FC	Fission chamber
FFM	Fix Filter Module
FFT	Fast Fourier Transform
FPGA	Field-Programmable Gate Array
ISTec	TÜV Rheinland ISTec GmbH – Institut für Sicherheitstechnologie
MFC	Miniature Fission Chamber
MCS	Multi-Channel Scaler
PC	Proportional Counter
PE	Polyethylene
PRM1	linear Power-Range channel Monitor 1
PSD	Power Spectral Density
SAD	Simultaneous Analog-Digital converter
TTL	Transistor-Transistor Logic
TUD	Technische Universität Dresden
U_{metal}	Metallic uranium
UO_2	Uranium oxide
VA	Vibrating Absorber
WP	Work package
WRM	Wide-Range channels Monitor (WRM1 and WRM2)

Summary

In the framework of the CORTEX project, the work package 2 targets the generation of high quality neutron noise experimental data for the subsequent validation of computer methods and models developed in work package 1. The AKR-2 reactor at TUD, and the CROCUS reactor at EPFL, are the experimental facilities where noise-specific experimental data are being generated. This report documents the experimental setup and measurements for each perturbation type and facility of the second campaigns. The raw time series will be distributed to the members of the consortium. The associated experimental results will be documented in separate internal reports and distributed to the members of the consortium.

1 Overview

The CORTEX project aims at developing an innovative core monitoring technique for anomaly detection in nuclear reactors, such as excessive vibrations of core internals, flow blockage, coolant inlet perturbations, etc. The technique will be based on primarily using the inherent fluctuations in neutron flux recorded by in-core and ex-core instrumentation, from which the anomalies will be differentiated depending on their type, location and characteristics. The method is non-intrusive and does not require any external perturbation of the system. The project will result in a deepened understanding of the physical processes involved. This will allow utilities to detect operational problems at a very early stage and to take proper actions before such problems have any adverse effect on plant safety and reliability.

The main purpose of the experimental campaigns at the AKR-2 and CROCUS reactors is to produce high quality noise-specific experimental data for the validation of the neutron noise computational models. The first campaigns were presented in [1], [2]. The present document is dedicated to the second campaigns, and is structured in two main sections: a first one describing the second experimental campaign at the AKR-2 reactor, and a second one describing the second experimental campaign at the CROCUS reactor. Following this report, all experimental data will be distributed to all partners in the form of time series identified by their measurement number, instrumentation, and signal's number.

For the 2nd measurement campaign at the AKR-2 at the TU Dresden 27 measurements were performed. During the measurements, absorbers of two different kinds perturbed the neutron flux of the reactor: singularly and both at once. The reactor response was recorded via 9 detectors: 2 fission chambers, 4 He-3 counters and 3 miniature scintillators. Compared with the first campaign, some advancements were realized, mainly based on the feedback of the modellers: two more detectors were in operation, with one fission chamber and the 3 miniature scintillators placed closer to the centre of the reactor. A new high precision linear motor axis was used as a vibrating absorber, allowing for a sinusoidal driving profile with a more flexible amplitude. The reactivity input was lowered by the use of indium foils as absorbing material instead of the cadmium foils used in the 1st campaign. The experimental channel 7 was blocked with polyethylene to facilitate the modelling with diffusion codes. Finally, two new data acquisition systems were used to record parts of the data.

At CROCUS, the fuel rods oscillation campaign focused on the reduction of uncertainties as compared to the first campaign. 31 experiments were carried out in total, which were measured using 15 detectors distributed within and around the core, as well as at distance. First, the power was increased from 100 mW to 1 W to increase the statistical significance, thanks to the use of fast electronics for the pulse mode detectors. Then the focus was set on long experiments (up to 4h continuously) with repeatability on a selected set of amplitude and frequency parameters: ±1.5 mm, and 0.1 and 1.0 Hz only. The additional detectors comprised two more large fission chambers, which allow high statistics and robust measurements, and two proportional counters made sensitive to the fast neutron component. Finally, more static and dynamic experiments were conducted without oscillations to allow for reference values. In addition, experiments were performed with equivalent perturbations of 9 and 1 rods but set at different positions, in order to target the discrimination of different spatial distributions.

2 AKR-2 second experimental campaign

In the week of the 6th July 2020 to the 10th July 2020, the 2nd CORTEX measurement campaign at the AKR-2 reactor at the TU Dresden was held. The TUD and EPFL project partners were present during the campaign.

For the perturbation of the reactor two different devices were available, used either separately or both at the same time. One acts as a vibrating absorber, where the absorber is driven by a linear motor axis and one as an absorber of variable strength, where the absorber is rotated by a stepper motor. The motion of the perturbation devices was recorded during the measurements. For the detection of the data, two fission chambers, four He-3 counters and three optical fiber based scintillator detectors were used. The signals were acquired via two FPGA-boards, two MCS and a mini-computer, called Beagle-Bone. The acquisition was started simultaneously for the MCSs and the TUD FPGA board, while the trigger signal was recorded on a dedicated channel for the Beagle-Bone and the EPFL FPGA.

27 measurements were performed during the course of five days. For 10 of the measurements, the perturbation was induced via the absorber of variable strength; for 14 with the vibrating absorber and for 3 measurements both devices were active at the same time. The recorded data are stored on the Chalmers FTP-server:

- Raw data can be found in the following folder:
  `/export/zh4/cortex/tud/Data_2nd_Campaign/raw_data/`
- Standardized time series data in txt format can be found in:
  `/export/zh4/cortex/tud/Data_2nd_Campaign/txt_data/`
- The naming convention for the txt files is as follows:
  `AKR2_`*`number of measurement_data acquisition system_number of detector`*
  (position signals for the rotating device and linear motor axis have detector numbers 10 and 11 respectively)

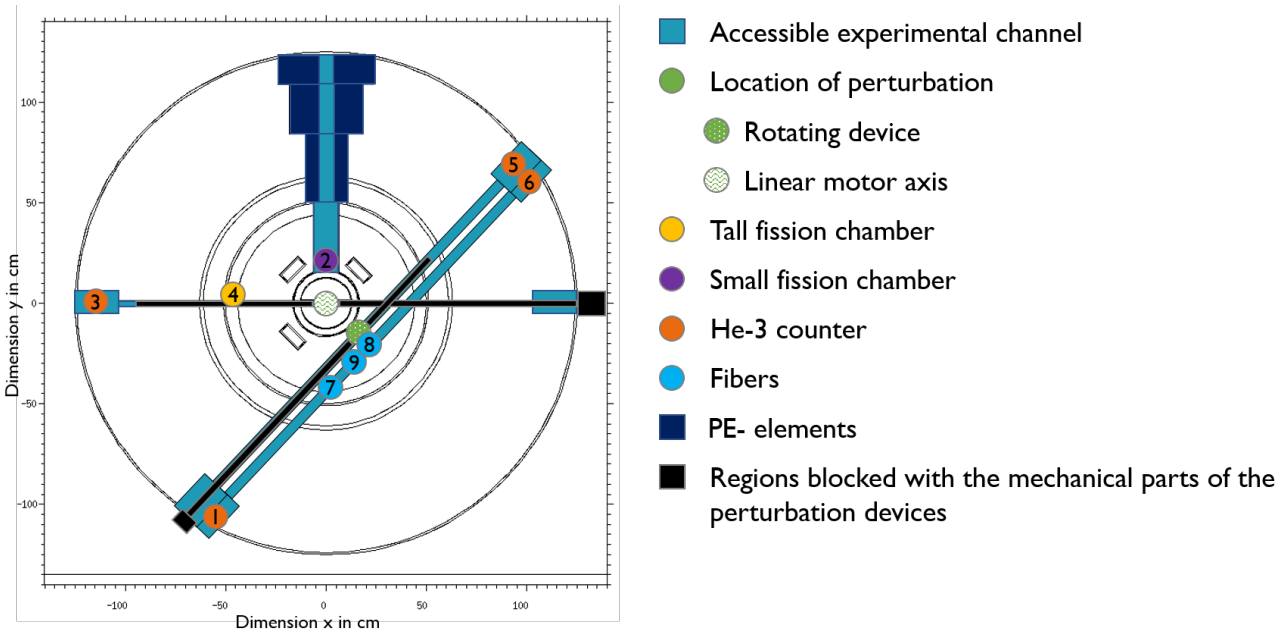

Figure 1: Overview of the setup of the 2nd measurement campaign

2.1 The AKR-2 reactor

The AKR-2 reactor, located at TU Dresden, is a thermal, zero-power reactor with an allowed maximum thermal operation power of 2 W. The core has cylindrical shape with a diameter of 250

mm and a height of 275 mm. The disk-shaped fuel elements consist of a homogeneous dispersion of polyethylene moderator and uranium oxide, which is enriched to 19.8 %. For security reasons the core is separable, with the lower half being movable. For the basic start-up procedure, the core halves are brought together. The operation is controlled by three control and safety rods installed next to the fuel zone, consisting of cadmium sheets on polyethylene blocks. A graphite reflector with approx. thickness of 32 cm surrounds the core. Underneath and above the core is about 25 cm and 70 cm graphite, respectively. The biological shield consists of two cylindrical walls of 15 cm and 58 cm thickness, made of paraffin and heavy concrete. The reactor is accessible via seven horizontal and two vertical experimental channels. The setup of the AKR-2 is illustrated in Figure 2. [3]

With respect to the first campaign, the main change to the reactor is that the tall central channel 7 was partially filled with polyethylene-elements, leaving just a cylindrical shaped hole with a diameter of 13 cm in the cylindrical part of the channel (see Figure 1).

The kinetics parameters of the reactor are known and were determined via MCNP and SERPENT calculations (for parameters see Table 8 in the annex). These simulations were successfully checked, over a selected frequency range, through the experimental determination of the reactors zero-power transfer-function (Figure 19) [4].

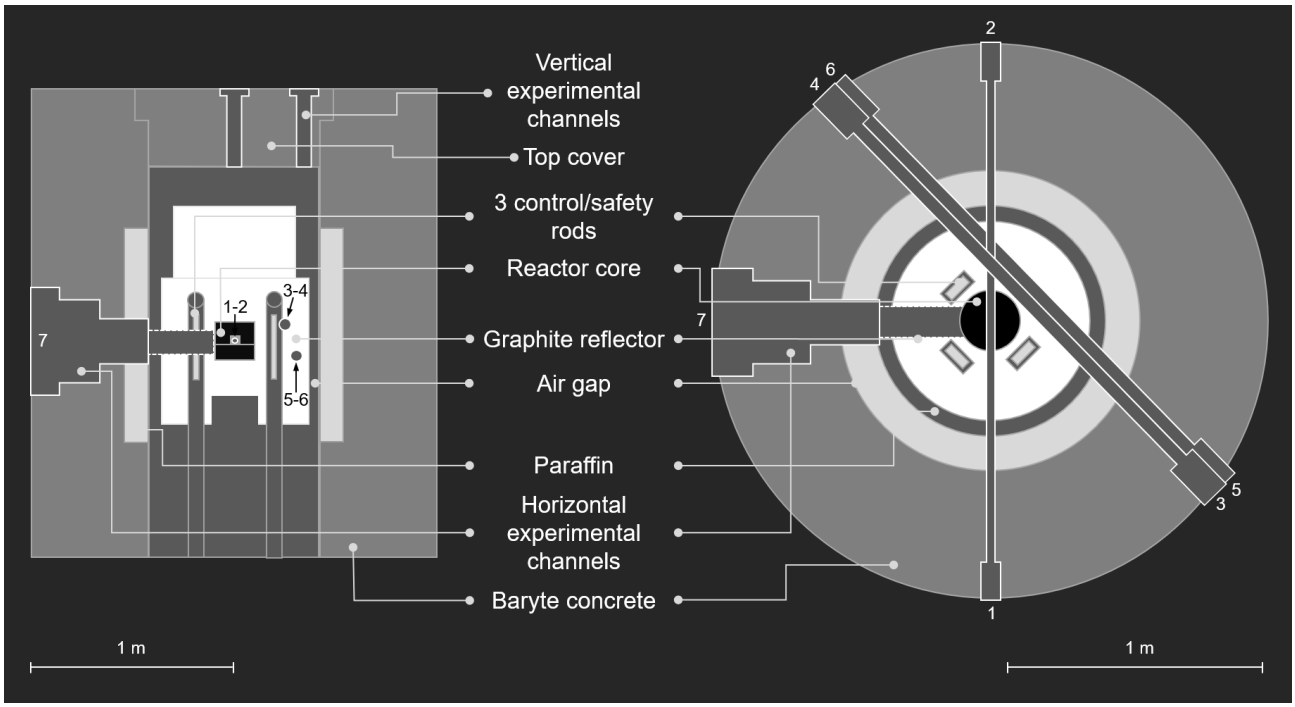

Figure 2: Schematic of the AKR-2 reactor.

2.2 Perturbation devices

During the second campaign, two different perturbation devices with motion control were involved. The technical devices to induce the reactivity perturbation can be differentiated by their technical application into a linear motor axis and a stepper motor driven rotating device. From a physics point of view the induced perturbation are like a vibrating absorber respectively an absorber of variable strength. The linear motor axis replaced the pneumatic pump of the 1st campaign, as it allows for a customizable driving profile and is more precise. Also the reactivity input of the perturbation was lowered by using indium instead of cadmium sheets as absorbers.

2.2.1 Vibrating absorber

The vibrating absorber triggers a repetitive perturbation in the reactor. For the 2nd AKR-2 CORTEX campaign this is realized using a linear motor axis, which moves a shaft containing an indium absorber within the experimental channel 1-2. The absorber is a stack of 13 indium foils with a diameter of 12.7 mm. The cumulative mass is 926.2 mg. It consists of high purity natural indium. The linear axis can be driven to reproduce different motion profiles. A sine like motion profile was chosen for the campaign. The maximum amplitude would be about 15 cm (for a total course of 30 cm for the absorber), respecting the safety limitations of the drive. For the experiments, amplitudes of 0.5 cm, 1 cm and 3 cm were used. The frequencies are limited at the lower end by the measurement time (minimum number of repetitions which was approximately 39 for the 2nd campaign) and at the upper end by the safety limitations of the axis, which allow a maximum frequency of 7 Hz. The principle of the setup is shown in Figure 3. The reactivity difference between the maximum and the minimum position of the absorber is different for different positioning types and can be seen in Table 1. It has to be mentioned, that the axis position is noted towards the internal axis position, in which the internal position encoder records the motion track. The absorber is at the centre of the core (0 in the coordinate system, in which the positions of the detectors are given in Table 2) for an axis position of 10.5 cm (compare maximum of graph in Figure 4). For the symmetrical perturbation around the centre of the core, the reactivity perturbation is of the order of the measurement error of the reactivity. The reactivity influence over the movement path was determined via compensation-method with help of one of the control and safety rods (rod no. 2). A relative position encoder records the movement of the axis.

Table 1: Reactivity of the VA for different positions

Position (axis internal) in cm	Position (reactor centre) in cm	Amplitude around position in cm	Min. pos. (reactor centre) in cm	Max. pos. (reactor centre) in cm	type	reactivity in cents ($/100)
14.5	4	± 0.5	3.5	4.5	small VA	0.5 ± 0.05
15	4.5	± 1	3.5	5.5	small VA	1,1 ± 0.05
15	4.5	± 0.5	4	5	small VA	0.5 ± 0.05
10.5	0	± 2	-2	2	symmetrical around centre of core	~ 0.05 to 0.1 ± 0.05
16	5.5	± 3	2.5	8.5	VA	3.35 ± 0.05

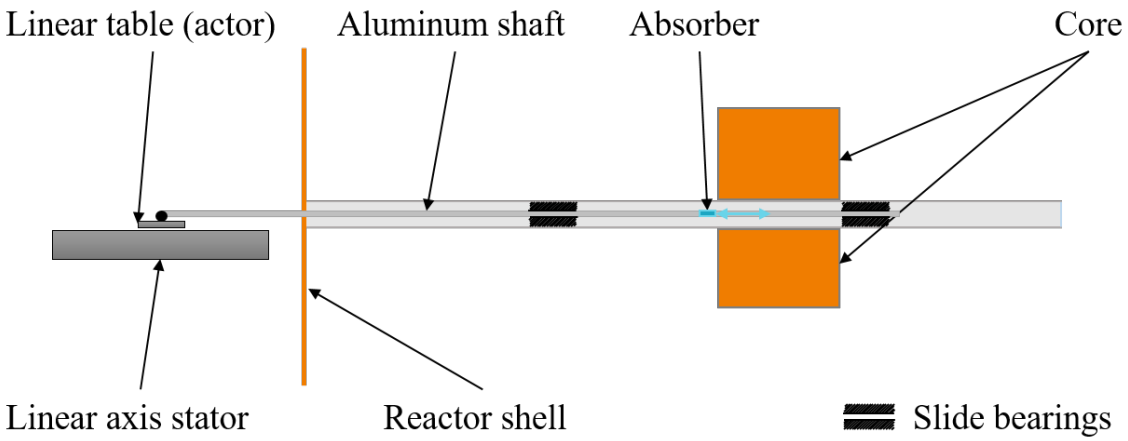

Figure 3: Schematic of the vibrating absorber

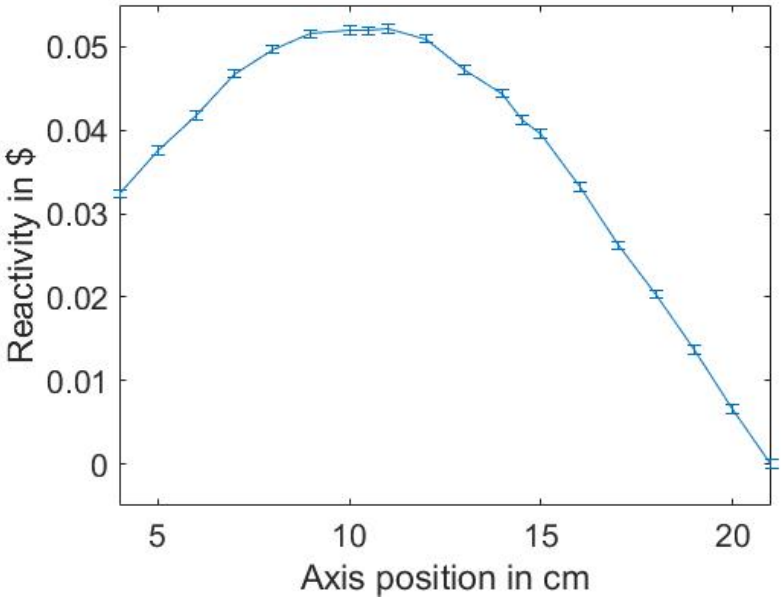

Figure 4: Reactivity of the vibrating absorber

2.2.2 Absorber of variable strength

The absorber of variable strength inserts a localized perturbation. For the 2nd CORTEX campaign at the AKR-2, this is realized with the help of an absorber, rotating in the experimental channel 3-4, driven by a stepper motor. The absorber is a bent rectangular cadmium sheet with dimensions of 25 cm x 2 cm x 0.02 cm with a bending and rotation radius of 2.98 cm. The largest dimension is parallel to the experimental channel. The material of the absorber is natural cadmium with unknown impurities.
The stepper motor induces a motion profile with a constant angular velocity. Frequencies range from 0.1 Hz to 4 Hz for the campaign. The lower frequency limit is set by the minimum width of the steps, resulting in a jerkily, stepwise movement at low frequencies. The perturbation is recorded at the 9 o'clock position (as can be seen in Figure 5). This position is referenced as angle 0°. In the current configuration, when the trigger is at position 0°, the absorber sheet is at 90° (phase shift between trigger and absorber is 90°). The movement direction is clockwise, seen from outside of the entrance 3 of the channel 3-4. The difference of the minimum and maximum reactivity during a rotation of the absorber is 0.022 $. The reactivity influence was determined in the same way as for the other absorber type. The reactivity over the angle is illustrated in Figure 5. The movement of the stepper motor was tracked with a positioning signal, every time the position trigger passed the 0° angle (absorber 90°).

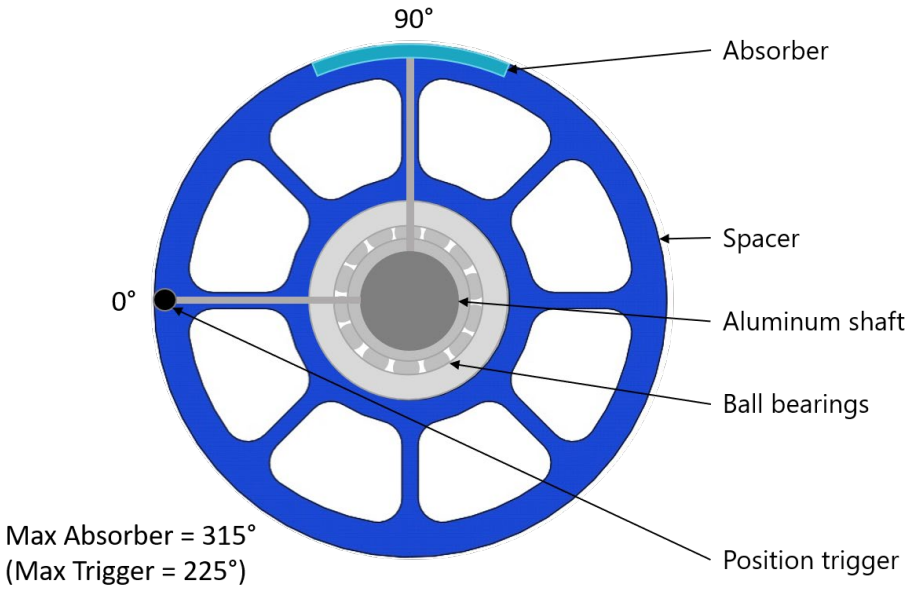

Figure 5: Schematic of the absorber of variable strength

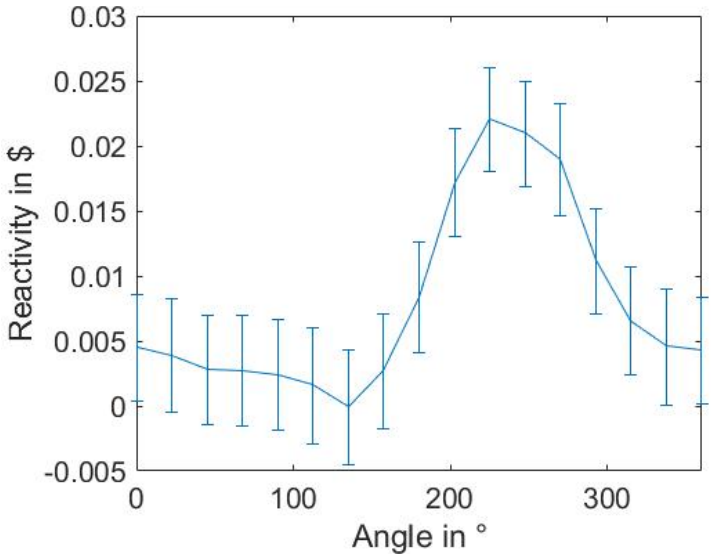

Figure 6: Reactivity of the absorber of variable strength regarding the position trigger

2.3 Neutron detection instrumentation

During the second campaign nine detectors were used. Three of them were of the fiber-type, which were newly developed by the EPFL [5]. The detectors, as well as the perturbations took place in the different horizontal experimental channels of the reactor, as these represent the only way to access the inner part of the AKR-2. The fiber detectors (7-9), as well as the fission chamber (2) were placed in close proximity to the reactor core. Also two new data acquisition systems were used. These are described in sections 2.3.2.2 and 2.3.2.4. Of the detectors permanently installed in the AKR-2 only detector 4 was used (same as in the 1st campaign).

2.3.1 Detectors

For the detection of the reactor's response to the perturbations, nine different detectors were used. One of them is permanently installed, to observe the reactor's operation, it is a relatively large fission chamber in pulse mode (4). Three of them are of the new fiber-type (7-9), developed within the

CORTEX project by the EPFL. Additionally, there are four He-3 counters (1, 3, 5, 6) and one relatively small fission chamber in pulse mode (2). More detailed information about the detectors can be found in Table 2 and in the Annex 6.2.

Table 2: Detectors in operation for the AKR-2 2nd measurement campaign

No	Type	Sensitive material	Position in relation to core centre (0° mid channel 7)		
			Height in cm	Radial in cm	Angle in °
1	PC	He gas	- 8 ± 2	104.4 ± 4	208.3 ± 0.5
2	FC	U coating	0 ± 2	17 ± 0.5	0 ± 0.2
3	PC	He gas	0 ± 2	102 ± 4	270 ± 0.2
4	FC	U coating	0 ± 2	48 $^{+0.5}_{-1.5}$	279 ± 3
5	PC	He gas	+ 8 ± 2	102.4 ± 4	57.4 ± 0.5
6	PC	He gas	- 8 ± 2	104.4 ± 4	61.7 ± 0.5
7	fiber	ZnS(Ag) with ^{6}Li	- 8 ± 2	42.4 ± 0.5	153.4 ± 1
8	fiber	ZnS(Ag) with ^{6}Li	- 8 ± 2	30 ± 0.5	135 ± 1
9	fiber	ZnS(Ag) with ^{6}Li	- 8 ± 2	31.6 ± 0.5	180 ± 1

2.3.2 Data acquisition systems

The TU Dresden used three different types of acquisition systems during the campaign. The first one comprises of two *ORTEC* multi-channel-scalers, which were already used for the last campaign and described in the deliverable 2.1 [1]. The second one is an FPGA-board using an in-house developed acquisition software; the third is a mini-computer called Beagle-Bone (BB). The fiber DAQ supplied by the EPFL consists of plastic optical fibers with neutron sensitive scintillators at their tips, silicon-photomultipliers, in-house developed amplifiers, and a CAEN V2495 unit as multi-channel scaler (see Section 3.3.2, p. 20). The setup of the DAQ can be seen in Figure 7; the designation of signals and their corresponding detector number and DAQ channel is presented in Table 3. The data acquisition was started with a trigger signal for the multi-channel scalers and the TUD FPGA. The Beagle-Bone and the EPFL DAQ recorded the trigger signal on a dedicated channel.

Table 3: Signals acquired by the AKR-2 2nd measurement campaign

Signal (No)	DAQ channel	Corresponding detector (No)
1	MCS 1	1
2	FPGA (TUD) 1	1
3	MCS 2	2
4	FPGA (TUD) 2	2
5	FPGA (TUD) 3	3
6	BB	4
7	FPGA (TUD) 5	5
8	FPGA (TUD) 6	6
9	CAEN FPGA (EPFL)	7
10	CAEN FPGA (EPFL)	8
11	CAEN FPGA (EPFL)	9

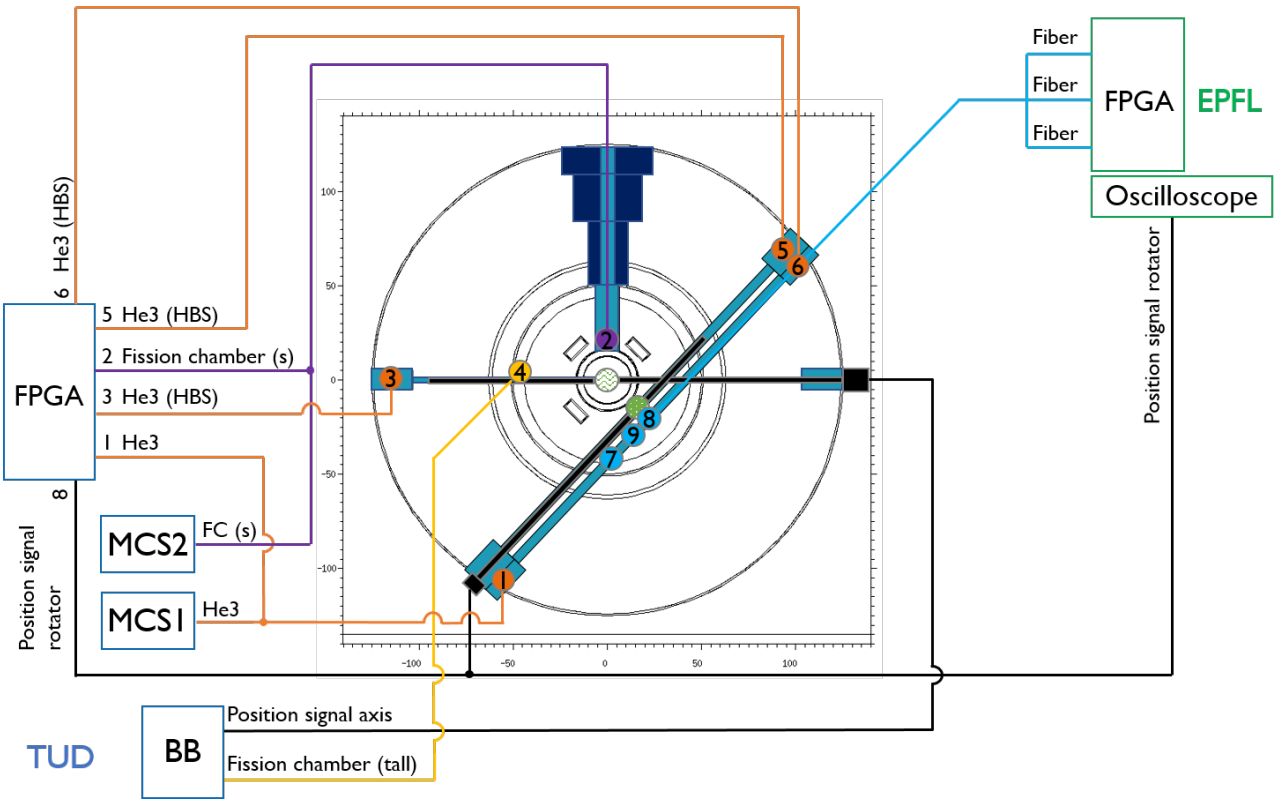

Figure 7: Connection of the signals with the DAQ

2.3.2.1 Multi-channel scalers

This acquisition system was already in use for the first campaign. The MCS have 65536 channels, which can acquire pulses without dead-time. Because of the limited number of channels, the cumulative time for each measurement is determined by the bin-width or dwell-time for each channel. The systems were tested and validated against an industrial type measurement system during the first campaign. The data acquisition of the MCS is started via the trigger signal.
The first MCS was used for data acquisition of detector 1, and the second MCS for data acquisition of detector 2 respectively. The data is saved in ASCII-files with the first column denoting the time step in seconds and the second column corresponding to counts. They are also provided in a standardized txt format (see section 2.3.3).

2.3.2.2 FPGA board

The FPGA-board has 8 BNC inputs for the acquisition of TTL-pulses. Additionally, there are trigger-in and trigger-out channels. The input-signal 1 acquired the signals of detector 1, the input-signal 2 acquired the signals of detector 2, the input-signal 3 acquired the signals of detector 3, the input-signal 5 acquired the signals of detector 5, the input-signal 6 acquired the signals of detector 6, and the input-signal 8 is the positioning signal of the rotating device.
The signals 1 and 2, which are already acquired via the MCS, are connected to the FPGA-board at the start of the 8th measurement. For the 9th and 10th measurement, no data could be acquired with the board, as it disconnected during the measurement. For the measurements 7 and 26, the signal of the detector 5 could not be stored.
The raw signals are saved in 32bit binary files containing the differences between individual neutron detection events in multiples of clock cycles of the FPGA (10 ns). Files can be converted to a human readable format using a python script located on the CORTEX ftp server at

`/export/zh4/cortex/tud/Data_2nd_Campaign/raw_data/bin_into_txt.py`.

All raw data files have also been converted to a standardized .txt files (see section 2.3.3)

2.3.2.3 Beagle-Bone

The mini-computer is able to acquire analogue signals. Therefore, it is used to store the signal of the detector 4 respectively the position signal of the relative motion encoder of the linear motor axis. The way of recording the trigger signal enables just the recording of one signal at once (detector 4 or the motion encoder). The signal of the detector 4 was transferred into current-mode via a *ROBOTRON* device, like in the 1st campaign for the ISTec signal acquisition.
The stored files contain in the first column a time-stamp, in the second the trigger level and in the third one the voltage level corresponding with the signal height of the detector respectively the relative motion encoder. They were also converted to a standardized txt format as described in section 2.3.3.

2.3.2.4 EPFL fiber analogue system

The EPFL DAQ system is based on Li 6 ZnS neutron scintillator crystals and plastic optical fibers, which guide the light to the silicon photo-multipliers (SiPM), generating electrical current signals. An EPFL developed preamplifier, shaper and discriminator board is used to generate voltage pulses and to discriminate background and gamma light pulses from neutron induced pulses, which are higher (after shaping). The signal is amplified using a Canberra 2022 amplifier and conditioned for counting by a Canberra 2030 single-channel analyser. The counting is performed using a CAEN V2495 FPGA logical unit and PC communication board CAEN V1718, stacked in a CAEN VME8008B crate. Dwell time is determined prior to start of the measurement. A series of ASCII text files are produced with counts per dwell time for each channel of the CAEN V2495. One of the channels was used to record the trigger signal, which is used to synchronize the measurements with other systems.

2.3.3 Standardized txt file format

All raw data was converted to a standardized txt file format in form of a time series (an example is depicted in Figure 8). The first line of the txt file contains a header with relevant information. Line 2 contains the dwell time followed by the detector signals. Due to interpolation of the signals or the analogue nature of the Beagle-Bone signal the detector values are floating point numbers.

The data can be found on the Chalmers ftp server in the folder:

```
/export/zh4/cortex/tud/Data_2nd_Campaign/txt_data
```

The files have the following naming convention:

```
AKR2_experiment number_data acquisition system_detector number.txt
```

The data acquisition systems are MCS, BB, FPGA, EPFL, FPGA-pos and BB-pos, where the last two refer to position signal and are assigned detector numbers 10 and 11.

```
# AKR-2 - det_01 - MCS - Measurement # 1 - Power (W) 1.5 - tw (s) 0.04 - tm (s) 2621.36 - expfreq (Hz) 2.0 - First value below corresponds to the dwell time (s)
0.04000
154.00000
168.00000
173.00000
172.00000
188.00000
135.00000
164.00000
170.00000
181.00000
179.00000
186.00000
187.00000
174.00000
162.00000
177.00000
181.00000
```

Figure 8: Example of the standardized txt format provided for the time series.

2.4 Experiments

In Table 4 the performed experiments are listed, separately for the absorber of variable strength and for the vibrating absorber and the experiments with both at once. All measurements were performed at reactor power of 1.5 W. The measurement time was determined by the limited number of channels of the MCS: 65536 resulting in measurement time of dwell-time times the channel number. A more detailed list, with active and non-active acquisition channels for each measurement can be found in Table 9 in the annex.

Table 4: List of experiments

Experiment No	Type	Frequency in Hz	Motion parameters in cm		Dwell-time in ms (MCS)	Measurement time in s (MCS)
			centre	amplitude		
1	AVS	2			40	2621.36
2	AVS	2			30	1966.02
3	AVS	0.1			30	1966.02
4	AVS	0.1			30	1966.02
5	AVS	4.5			30	1966.02
6	AVS	4.5			30	1966.02
7	AVS	1			30	1966.02
8	AVS	2			30	1966.02
9	VA	2	14.5	0.5	30	1966.02
10	VA	0.1	14.5	0.5	30	1966.02
11	VA	7	15	1	30	1966.02
12	VA	0.01	15	0.5	60	3932.04
13	VA	0.01	15	0.5	60	3932.04
14	AVS	2			40	2621.36
15	VA	0.01	10.5	2	60	3932.04
16	VA	0.01	10.5	2	60	3932.04
17	VA	1	10.5	2	30	1966.02
18	VA	1	10.5	2	30	1966.02
19	VA	4	16	3	30	1966.02
20	VA	2	16	3	30	1966.02
21	AVS	2			30	1966.02
22	VA	2	16	4	30	1966.02
23	VA + AVS	2	14.5	0.5	30	1966.02
24	VA + AVS	0.1	14.5	0.5	60	3932.04
25	VA	0.1	14.5	0.5	30	1966.02
26	VA + AVS	2	16	3	30	1966.02
27	VA	0.1	14.5	0.5	30	1966.02

For the measurement 17 all neutron detector signals may show unexpected behaviour as the axis stopped moving during the measurement. For the measurement 20, just the first 20 min should be considered for evaluation, as the absorber of variable strength (which was not supposed to be used) was accidentally moved at that time.

3 CROCUS second experimental campaign

The second experimental campaign in the CROCUS reactor took place from 9 to 22 October 2019. Vibrating fuel rods experiments were carried out using an in-core device that was specifically developed for that purpose within the COLIBRI program (CROCUS Oscillator for Lateral Increase Between u-metal Rods and Inner zone). This section describes the CROCUS reactor, the COLIBRI device and the vibrating fuel rods experiments. It is to be noted that aside from the detection setup, the reactor configuration remains the same than for the first campaign.

3.1 The CROCUS reactor

CROCUS is an experimental zero-power reactor, uranium-fueled and water-moderated, dedicated to teaching radiation and reactor physics, and to research. It is located at the École Polytechnique Fédérale de Lausanne (EPFL) and it has been licensed for operating at a maximum power of 100 W, i.e. a total neutron flux of ~2.5×10^9 n/cm^2/s at the core center. Criticality is controlled either by changing the core's water level using a spillway, or by two B_4C absorber control rods, with an accuracy of ±0.1 mm (equivalent to approximately ±0.4 pcm) and ±0.5 mm, respectively. CROCUS operates at room temperature using a controlled water loop with secondary and tertiary circuits, two heat exchangers and an electrical heater.

The core is located in an aluminum vessel of 130 cm in diameter and 1.2 cm in thickness. It is filled with demineralized light water, acting as both moderator and reflector. Its active part has the approximate shape of a cylinder of about 60 cm in diameter and 1 m in height. It consists of two interlocked fuel zones with square lattices of different pitches: an inner zone of 336 UO_2 rods with an enrichment of 1.806 wt.% and a pitch of 1.837 cm; an outer zone of 172 U_{metal} rods in nominal configuration, 0.947 wt.% and 2.917 cm; a varying water gap between the two zones because of the two different pitches. The picture of the facility and critical assembly configuration is shown on Figure 9. Both uranium fuels consist of a 1-m pile of cylindrical pellets cladded in aluminum. The rods are maintained vertically by two octagonal aluminum grid plates spaced 1 m apart. The grids have a 0.5-mm cadmium layer to limit axial neutron leakage to the environment, i.e. structures activation, with the active zone of the fuel starting above the lower cadmium layer.

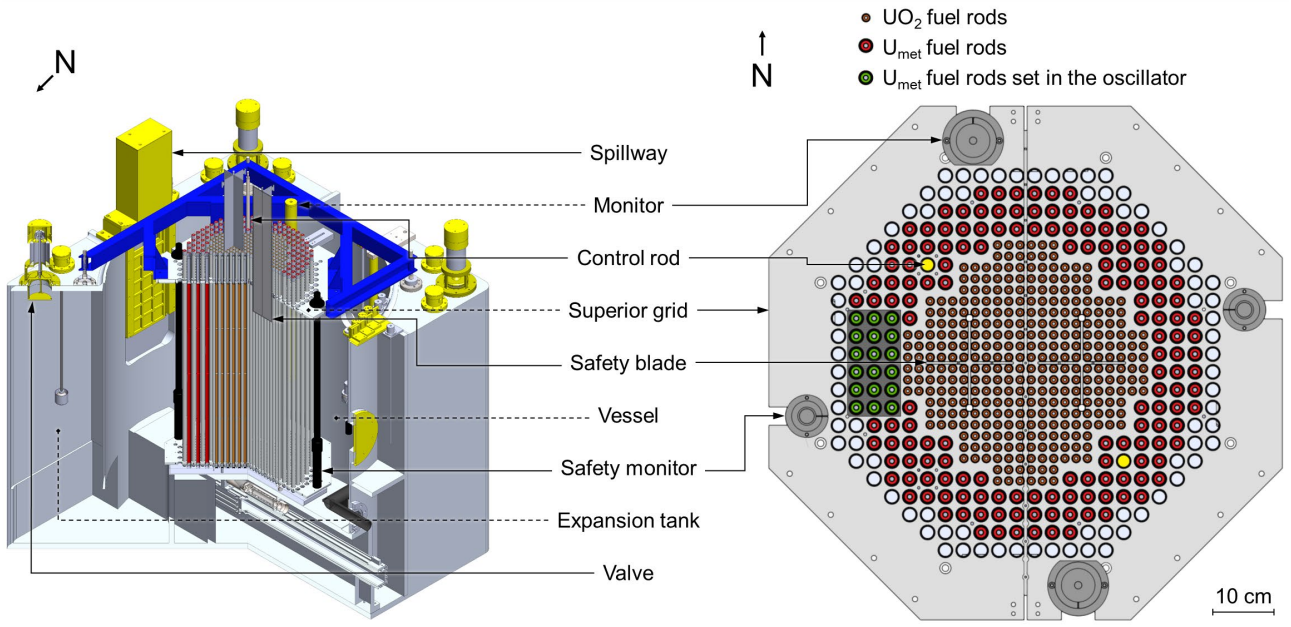

(a) Core structure and internals, isometric view (b) Upper grid and fuel lattice

Figure 9 – The CROCUS reactor: isometric view of the vessel (left), and top view of the core superior grid and configuration, with the indication of the location of the fuel rods set in the oscillator (green).

3.2 The fuel rods oscillator

The COLIBRI fuel rods oscillator is designed to oscillate simultaneously any of 18 metallic uranium fuel rods laterally in the west region of the core periphery zone. It consists in two moving plates set above and below the core grids, and rigidly connected by an aluminum beam (see Figure 10). Each one carries an extremity of the fuel rods, top and bottom respectively.

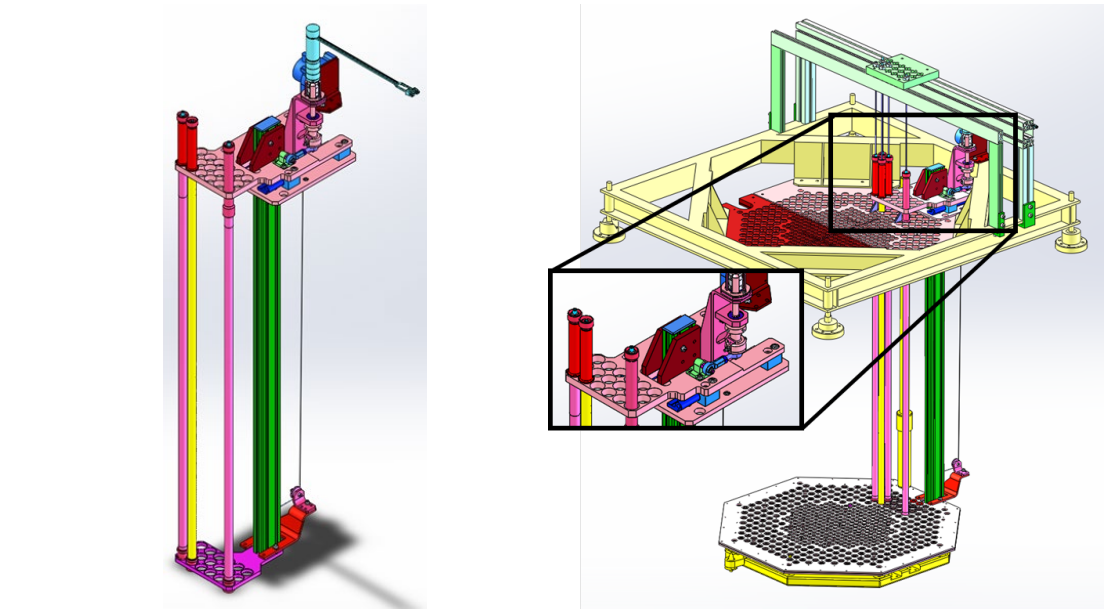

Figure 10 – COLIBRI fuel rods oscillator alone (left) and with core structures (right), and a few rods inserted in the device.

The top moving plate is fixed on the superior grid via gliders. Its oscillation is produced by a motor: the motor rotation is converted to a linear translation using an eccentric sheave and a rod. The oscillation is transferred to the bottom moving plate *via* the aluminum beam. The bottom moving plate is free of movement except for the connection to the transmission beam (no gliders).

New grids were produced for hosting the oscillator. Aside from the enlarged holes at COLIBRI's location, the cadmium layer set in sandwich in each grid was increased to 1-mm thickness instead of 0.5 mm (see Figure 11 and Figure 12). Other mechanical parts, such as those far in the reflector, or above and below the grids, are not detailed in this document as they are not relevant for the modeling.

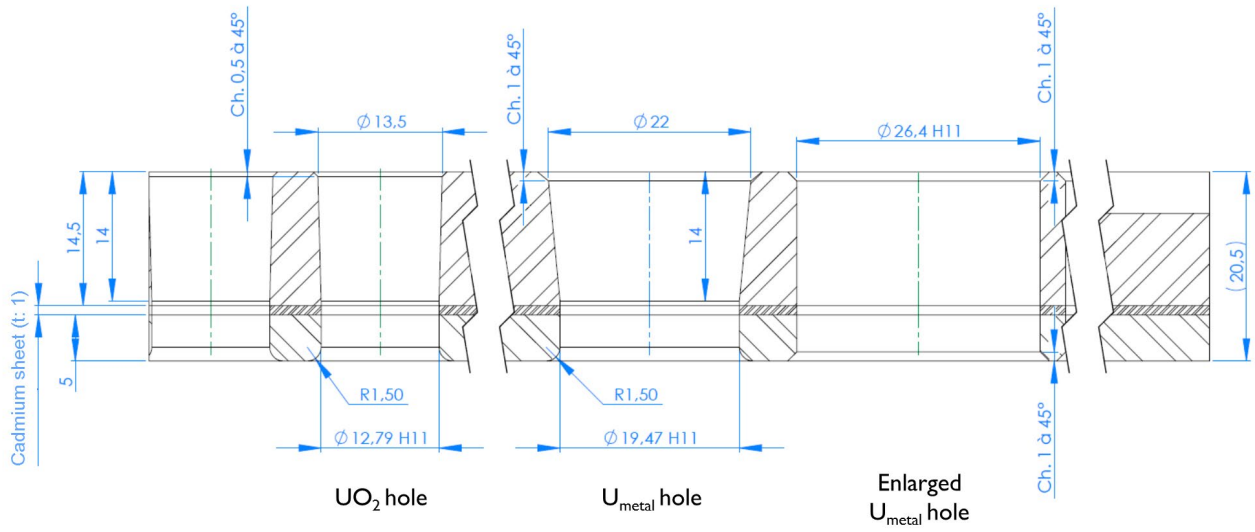

Figure 11 – Cross section of the modified superior grid: enlarged holes in COLIBRI's region and thicker cadmium layer (1 mm).

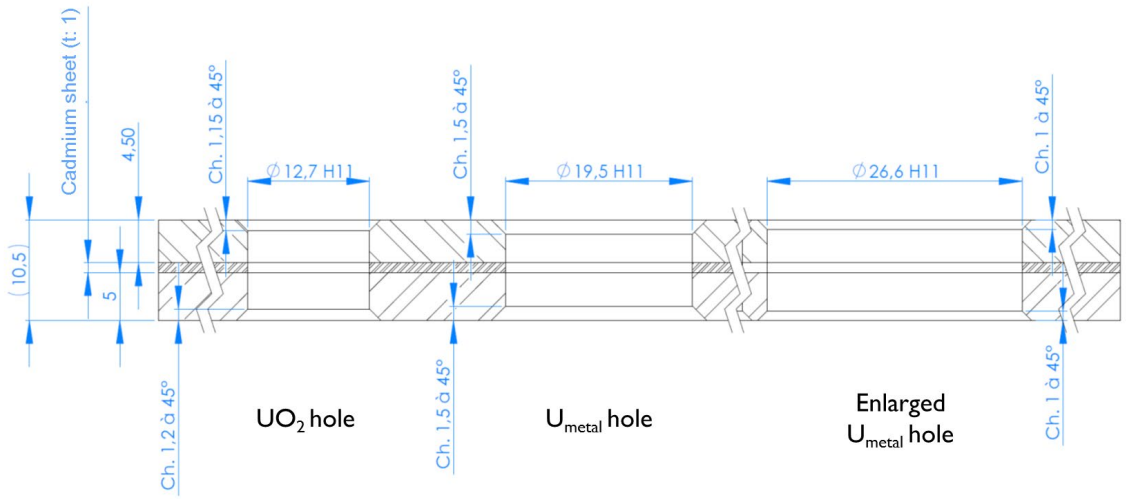

Figure 12 – Cross section of the modified inferior grid: enlarged holes in COLIBRI's region and thicker cadmium layer (1 mm).

The selection of the moving fuel rods is performed by leaving them laying on the reactor base plate (non-moving), or suspending them up 10 mm above the base plate to insert them in the moving plates. Top and bottom end caps are fixed to each rod to allow the insertion in the enlarged holes of either the static grids or the moving plates (see Figure 13). The weight of the oscillating rods is supported by a platform. The amplitude of the oscillation is precisely tuned by changing the eccentricity of the sheave with calibration plates, 0.5 mm by 0.5 mm from 0 to ±3 mm in theory. Its frequency is depending on the speed of the motor, with a fixed conversion factor.

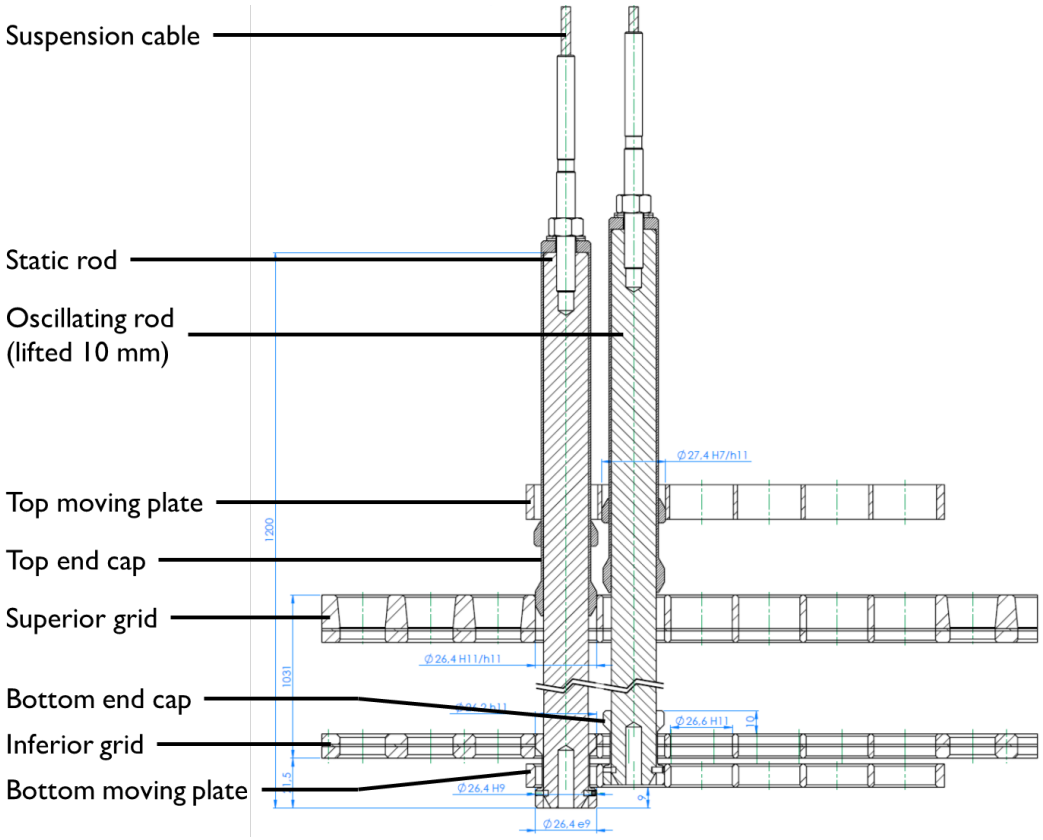

Figure 13 – Side cross section of the oscillator with only two fuel rods inserted in it; one fuel rod is in its static configuration laying at the bottom (left), the other one is lifted up 10 mm for oscillation.

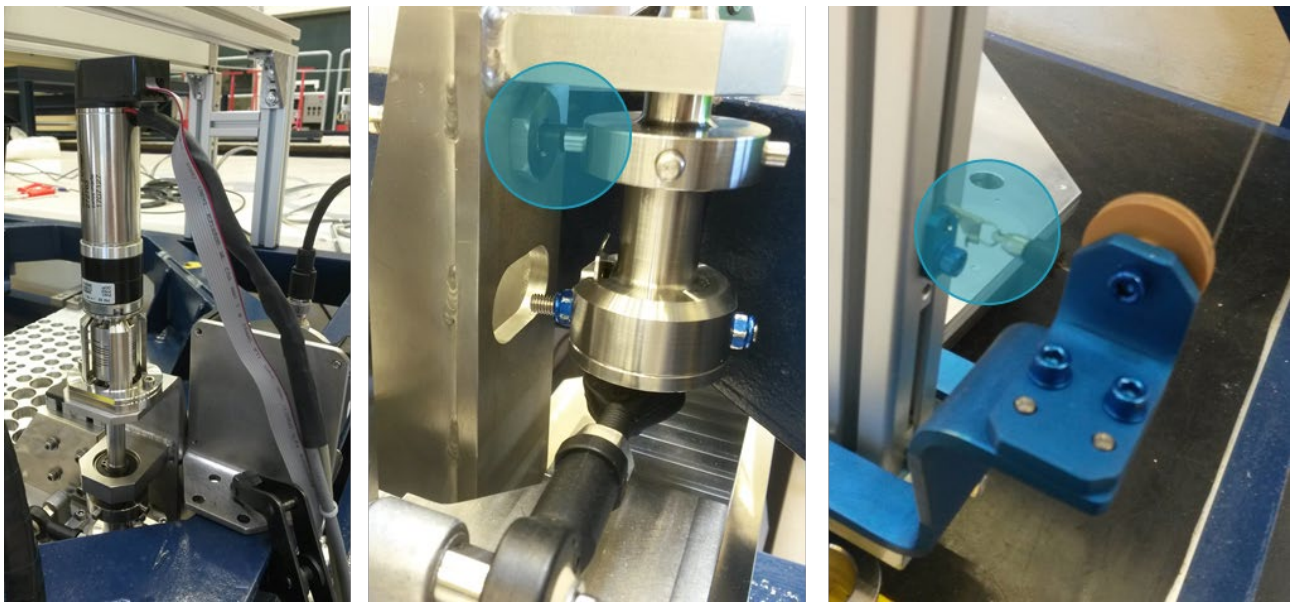

Figure 14 – Details of the control and monitors of the oscillation: (left) Motor on its rotation axis; (center) Close-up on the rotation axis with focus (blue) on the inductive captor detecting one of the four pins; (right) Measuring cable and close-up (blue) on its connection at the bottom to the transmission aluminum beam.

The oscillation is controlled and monitored *via* a LabVIEW-based software. An inductive captor is set at the rotation axis (i.e. at the top), which detects the actual movement of the motor by detecting the passage of four metallic pins per rotation. A cable coder is used to measure the displacement of the moving plate, i.e. at the bottom, with a 0.1 mm precision. These features are presented in Figure 14. The software provides as a csv file output the recording of the motor position and speed, the signal of the inductive captor, and the measurement of the cable, with 10 ms time-steps. A typical recording of an oscillation is presented in Figure 15. The inductive captor signal is also extracted for live and synchronized recording with the detection instrumentation.

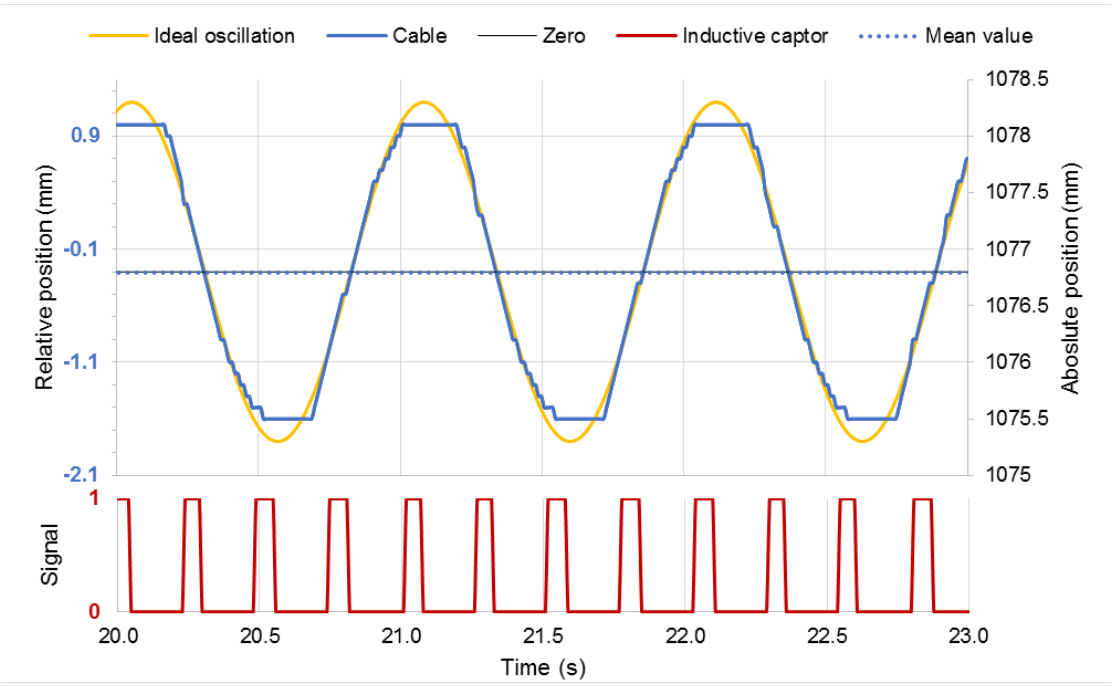

Figure 15 – Typical inductive captor (bottom, red) and cable (top, blue) signals, here in the case of one rod oscillating in air at ±1.5 mm and 1 Hz. In yellow, ideal sinusoidal oscillation for comparison with the real and measured displacement. The mean of the signal and the zero, which corresponds to the rods' nominal position, are also represented.

The behavior of the oscillator has been characterized in air and in water, out of the vessel and in-core, empty, 1-rod and 18-rods loaded. The behavior in frequency is sound. In amplitude, the device is rigid at the top, depending only on the rotation to translation conversion: a 0.1 mm flattening of the sinusoid due to mechanical plays in the crank and rod is expected (see Figure 15). The results on the oscillation amplitude at the bottom are presented in Figure 16. It demonstrates inertia effects inducing an increase of the amplitude for the full 18-rods load case and above 1 Hz, which is the case of the measurement campaign described in this report. This effect cannot be corrected, and thus has to be taken into account as is.

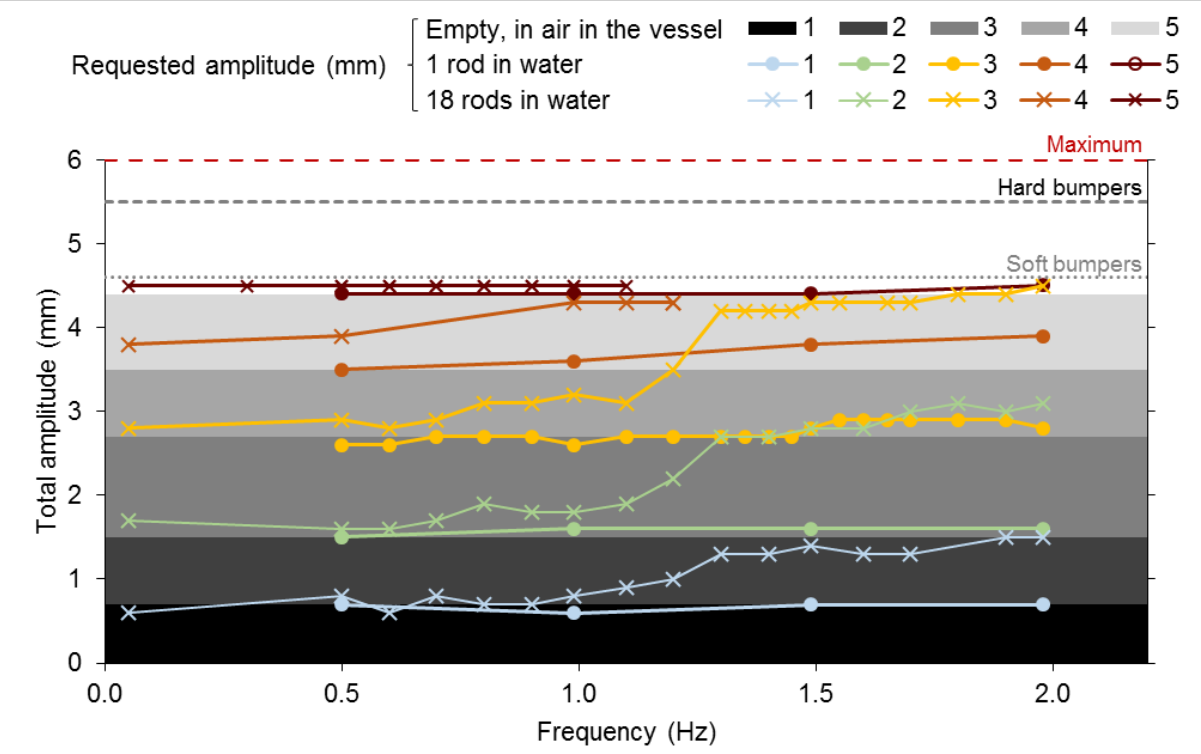

Figure 16 – Comparison of the oscillator behavior at the bottom position for 1 and 18 rods loads in water (1000 mm), as compared to the device oscillating empty loaded in air (i.e. expected to be equivalent to the behavior of the top part). All measurements were carried out using the cable coder.

3.3 Neutron detection instrumentation

3.3.1 Detectors

The detection instrumentation comprised the facility monitors, and different types of additional ex-core and in-core detectors, for a total of fifteen detectors of various sizes and sensitivities. Changes with respect to the first campaign are stressed in bold:

- Two safety monitors ^{235}U-coated fission chambers: Photonis CFUM21,
- Two operation monitors ^{10}B-coated compensated ionization chambers: Merlin-Gerin CC54,
- Two in-core small BF_3 proportional counters: Transcommerce International MN-1,
- Two in-core smaller BF_3 proportional counters: unknown brand and model,
- **Two additional** ex-core ^{3}He proportional counters: Canberra 12NH25/1F,
- **Four instead of two** ex-core large ^{235}U-coated fission chambers: Photonis CFUL01,
- One in-core ^{235}U-coated miniature fission chamber: Photonis CFUF34,

All detectors are based on prompt detection processes. The specification and location of each of them with regards to the core and COLIBRI are presented in Table 5 and Figure 17, and with respect to the MCNP model – coordinates and universes. All four monitor detectors are set at unchanged reference positions, as presented in the CROCUS benchmark [6] and models (all available on the ECCP). The other detectors specifications, such as sensitive area and channels dimensions, are included in the Appendix 6.3, p. 30. Their sensitive area were set vertically at core mid-height, but for the ^{3}He proportional counters (detectors 9 and 10). On the horizontal plane, for the majority of them the location was updated as compared to the first campaign. The now four (instead of two

during the first campaign) large CFUL01 FC were set in the reflector at all four cardinal positions, including west, closest to COLIBRI. The BF_3 counters were set at positions within the lattice as presented in Figure 17, in the control rod guide tubes for the NW and SE ones (detectors 5 and 7), and in aluminum channels for the other two (detectors 6 and 8). The miniature fission chamber was set at core center. The two additional ^{3}He detectors were set in a sheath of polyethylene and cadmium in order to cut their sensitivity to thermal neutrons (Cd), and enhance their sensitivity to fast neutrons (PE). The general uncertainty on detector position is ±1 mm, except for detectors 9 and 10 (^{3}He detectors), for which it is ±5 mm.

Table 5 – Detectors specifications and locations with respect to the MCNP model coordinates. In italic, location coordinates within the lattice.

	Detector					Acquisition		Location (cm)		
#	Type	Brand	Model	Sensitive material	Approximate sensitivity	DAQ	Channel	East	North	MCNP
1	FC	Photonis	CFUM21	^{235}U coating	10^{-2} n_{th}^{-1}	V2495	96	+35.8	+8.7	u = 31
2	FC	Photonis	CFUM21	^{235}U coating	10^{-2} n_{th}^{-1}	V2495	97	-35.8	-8.7	u = 31
3	CIC	Merlin-Gerin	CC54	^{10}B coating	3×10^{-14} $A.n_{th}^{-1}$	HDO6104A	3	-8.6	+36.35	u = 30
4	CIC	Merlin-Gerin	CC54	^{10}B coating	3×10^{-14} $A.n_{th}^{-1}$	WaveSurfer10	3	+8.6	-36.35	u = 30
5	PC	-	-	$^{10}BF_3$ gas	10^{-2} n_{th}^{-1}	V2495	64	*-16.0*	*16.0*	-
6	PC	Trans. Int.	MN-1	$^{10}BF_3$ gas	10^{-2} n_{th}^{-1}	V2495	65	*27.7*	*10.2*	u = 21
7	PC	-	-	$^{10}BF_3$ gas	10^{-2} n_{th}^{-1}	V2495	66	*16.0*	*-16.0*	-
8	PC	Trans. Int.	MN-1	$^{10}BF_3$ gas	10^{-2} n_{th}^{-1}	V2495	67	*-27.7*	*-10.2*	u = 21
9	PC	Canberra	12NH25/1F	^{3}He gas	-	V2495	68	+106.9	-25.0	-
10	PC	Canberra	12NH25/1F	^{3}He gas	-	V2495	69	-106.9	+25.0	-
11	FC	Photonis	CFUL01	^{235}U coating	1 n_{th}^{-1}	HDO6104A	1	-14.6	+29.5	-
12	FC	Photonis	CFUL01	^{235}U coating	1 n_{th}^{-1}	HDO6104A	2	+32.4	+2.8	-
13	FC	Photonis	CFUL01	^{235}U coating	1 n_{th}^{-1}	WaveSurfer10	1	-14.7	-29.5	-
14	FC	Photonis	CFUL01	^{235}U coating	1 n_{th}^{-1}	WaveSurfer10	2	-33.1	-2.5	-
15	MFC	Photonis	CFUF34	^{235}U coating	10^{-3} n_{th}^{-1}	V2495	98	0	0	-

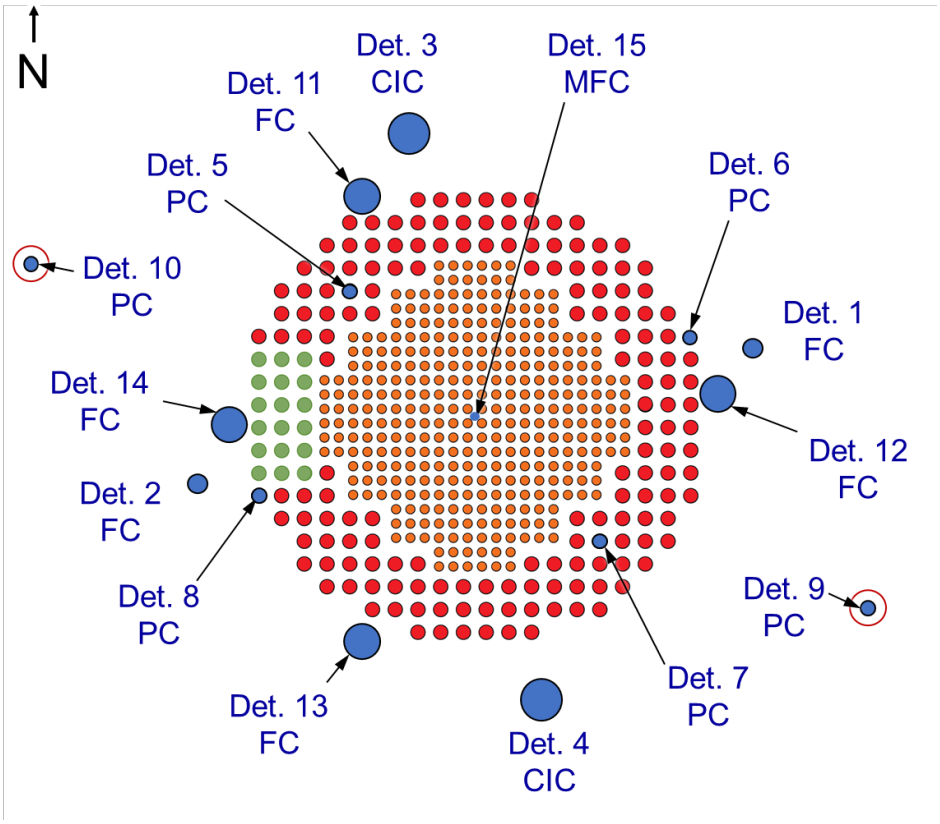

Figure 17 – Experimental setup of detectors.

3.3.2 Data acquisition systems

The operation ionization chambers and the large CFUL01 fission chambers were operated in current mode, whereas all the other detectors were operated in pulse mode. The detectors and their electronics were connected to three different data acquisition systems: two oscilloscopes for the current mode, and an FPGA programmable board for the pulse mode. All three systems were synchronized thanks to a start trigger, and recorded the inductive captor signal for allowing synchronization to the mechanical perturbation. In addition, the safety monitors were used in MCS mode for power monitoring using Canberra DSA-1000 data acquisition systems with the Genie2000 software.

3.3.2.1 Current mode acquisition systems

Two current mode acquisition systems were used for recording the CIC monitors (detectors 3 and 4), and the large CFUL01 fission chambers (detectors 11 to 14). They consist in in-house current amplifiers, which outputs were distributed between two Teledyne Lecroy oscilloscopes, namely a Wavesurfer 10, and an HDO6104A. The amplification scheme is depicted in Figure 18.

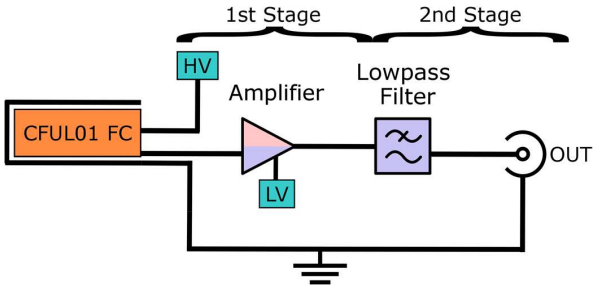

Figure 18 – Schematic of the in-house developed current amplifier connected to a typical large FC Photonis CFUL01, such as those used during the CROCUS campaign (detectors 11 to 14).

3.3.2.2 Pulse mode acquisition system

All pulse mode signals were recorded using an FPGA board from CAEN, namely the V2495. Detectors 5 to 10, i.e. all proportional counters, used CAEN low noise fast preamplification kits consisting in an A1427 preamplifier and an A1428 discriminator. The detector 15 miniature fission chamber used standard preamplifier (Tennelec 2025) and amplifier (Canberra 2022).

3.4 Experiments

The goal of the campaign was a better observation of spatial effects, mainly through uncertainty reduction. Three types of experiments were carried out for that purpose: static, dynamic, and in oscillation:

- Static: determination of the critical configuration of extremal and nominal positions of rods within the oscillator, as well as corresponding signal in the detectors,
- Dynamic: verification of detectors' linearity, and assessment of reactivity via period,
- Oscillation: first longer measurements for one selected amplitude (±1.5 mm) and two frequencies (0.1 and 1.0 Hz) of 18 oscillated rods; secondly experiments with reduced and same number of oscillated rods but placed differently.

The reactor was operated with the water level, contrary to the first campaign, in order to allow more in-core detectors by using both control rod guide tubes (see Figure 17). The global reactivity effect of the oscillations was compensated to follow a stable power. In practice, the oscillation was started first, then the reactor was stabilized in power with the water level before starting the measurements. The water level was updated along the experiments. The water temperature was controlled at 20.0 ± 0.1 °C. Following linearity tests, and thanks to the fast pulse mode electronics, the power was set around a higher power of 1 W, allowing up to ten times better detection statistics than for the first campaign.

The list of all experiments is presented in

Table 7 (see next page) with their identification number. 31 experiments were carried out in total, with redundancy, both for testing and repeatability purposes. Until experiment 16, all 18 rods were lifted in the oscillation position: in the static case, the motor was off and the position was set at positions of interest, either in their nominal position within the lattice, or extremal positions. For the following experiments, only part of the rods were selected: the selected rods are identified in Table 6 below. In a first step, 9 rods were selected: 9 on the North, then 9 on the South. In a second step, only one rod was selected, North, then South.

Table 6 – Identification of rods within the fuel rods oscillator.

	North		
	A	B	C
1	O	O	O
2	O	O	O
3	O	O	O
4	O	O	O
5	O	O	O
6	O	O	O

All oscillation experiments were acquired by all three acquisition systems, which were synchronized using a trigger. The duration of each measurement was maximized so as to reduce uncertainties as well, well above the first campaign.

Table 7 includes the oscillation specifications as well as the final control rod position, and water level oscillation. Waves at the surface of the water induced by oscillations were still measured using the reactor instrumentation (INUS ultrasonic sensor). The indicated values correspond to the maximum range observed. The fuel rods oscillation is described in requested amplitude and frequency. For the static measurements, the selected rods position is indicated.

The experimental data can be found on the Chalmers ftp server in the folder:

/export/zh4/cortex/epfl/Experimental data

The files have the following naming convention:

CROCUS_experiment number_data acquisition system_detector number.txt

Table 7 – Experiments list with corresponding reactor state (including final position of water level, and water level oscillations' amplitude), and oscillation specifications (rods, amplitude or position, frequency, and ID).

Experiment				Reactor				Setup			
#	Type	Date	Start	Duration	Power	Water level	Water osc.	Rods	Req. amp. or position	Freq.	Osc. ID
				s	mW	mm	mm	mm	mm	Hz	
1	**Oscillation**	**09.10.19**	**18:17**	**1000**	**500**	**966,80**	**0,10**	All	**±1,5**	**0,49**	**1**
2	**Oscillation**	**10.10.19**	**11:03**	**5000**	**1100**	**966,10**	**0,20**	**All**	**±1,5**	**0,97**	**2**
3	Linearity	10.10.19	13:22	-	↘ 100	956,00		All	0		
4	Linearity	10.10.19	14:48	-	↗ 900	-		All	-		
5	**Oscillation**	**10.10.19**	**15:35**	**5000**	**900**	**966,60**	**0,10**	**All**	**±1,5**	**0,10**	**3**
6	**Oscillation**	**10.10.19**	**17:27**	**5000**	**900**	**966,50**	**0,20**	**All**	**±1,5**	**0,97**	**4**
7	**Oscillation**	**11.10.19**	**10:04**	**15000**	**1000**	**966,50**	**0,00**	**All**	**±1,5**	**0,10**	**5**
8	**Oscillation**	**11.10.19**	**15:37**	**15000**	**960**	**966,60**	**0,30**	**All**	**±1,5**	**0,97**	**6**
9	Background	14.10.19		-	-	500,00		All	-		
10	Background	14.10.19		-	-	500,00		All	-		
11	Linearity	14.10.19	10:46	-	↗ 1000	-		All	-		
12	Static	14.10.19	11:19	1000	1000	967,00		All	-1,5		
13	**Oscillation**	**14.10.19**	**11:53**	**1000**	**1000**	**966,40**	**-**	**All**	**±1,5**	**0,10**	**7**
14	Static	14.10.19	14:39	1000	1000	967,00	0,05	All	0		
15	Period	14.10.19	15:10	2000	100 ↗	966,60		All	-1,5		
16	Static	15.10.19	09:31	1000	1000	966,00		All	+1,5		
17	Static	17.10.19	11:13	1000	1000	967,00		A1-C3	-1,5		
18	**Oscillation**	**17.10.19**	**12:17**	**5000**	**1000**	**967,05**	**0,10**	**A1-C3**	**±1,5**	**0,97**	**8**
19	Background	17.10.19	00:00	0	-	500,00		A1-C3	-		
20	Background	17.10.19	00:00	0	-	500,00		A1-C3	-		
21	Linearity	17.10.19	00:00	0	0 ↗	-		A4-C6			
22	Static	17.10.19	14:57	1000	1000	967,10		A4-C6	-1,5		
23	Static	18.10.19	10:57	1000	1000	967,35		A4-C6	-1,5		
24	**Oscillation**	**18.10.19**	**11:36**	**5000**	**1000**	**967,05**	**0,10**	**A4-C6**	**±1,5**	**0,97**	**9**
25	Linearity	18.10.19		0	-	-		C1	-1,5		
26	Static	18.10.19	15:13	1000	1000	967,35		C1	-1,5		
27	**Oscillation**	**18.10.19**	**15:49**	**5000**	**1000**	**967,50**	**0,10**	**C1**	**±1,5**	**0,97**	**10**
28	Shutdown	18.10.19	00:00	0	1000 ↘	-		C1	-		
29	Linearity	22.10.19	00:00	0	0 ↗	-		C6	-1,5		
30	Static	22.10.19	09:46	1000	1000	966,60		C6	-1,5		
31	**Oscillation**	**22.10.19**	**10:30**	**5000**	**1000**	**966,70**	**0,10**	**C6**	**±1,5**	**0,97**	**11**

4 Conclusion

In the framework of the CORTEX project, the work package 2 targets the generation of high quality neutron noise experimental data for the subsequent validation of computers methods and models developed in work package 1.

In this aim, the second campaigns in the TUD AKR-2 and EPFL CROCUS zero power experimental reactors were successfully carried out in July 2020 and October 2019. It consisted in measurements in reference static states, and with mechanical perturbations arising from rotating and vibrating absorbers, and from vibrating fuel rods, respectively. The present report documents the experimental setups and measurements for each facility and perturbation type. The experimental time series have been made available to the members of the consortium through the Chalmers FTP server.

Following this report, the experimental results will be prepared and distributed to the members of the consortium in the form of an internal report containing PSD powers and phase for each experiment, perturbation and detector.

5 References

[1] V. Lamirand, M. Hursin, A. Rais, S. Hübner, C. Lange, J. Pohlus, U. Paquee, C. Pohl, O. Pakari, and A. Laureau, "Experimental report of the 1st campaign at AKR-2 and CROCUS," CORTEX Deliverable 2.1, 2018.

[2] V. Lamirand, A. Rais, S. Hübner, C. Lange, J. Pohlus, U. Paquee, C. Pohl, O. Pakari, P. Frajtag, D. Godat, M. Hursin, A. Laureau, G. Perret, C. Fiorina, and A. Pautz, "Neutron noise experiments in the AKR-2 and CROCUS reactors for the European project CORTEX," *EPJ Web Conf.*, vol. 225, p. 04023, Jan. 2020.

[3] B. Boehmer, M. Grantz, W. Hansen, D. Hinke, J. Konheiser, H.-C. Mehner, K. Noack, R. Schneider, I. Stephan, and S. Unholzer, "Investigation of Gamma and Neutron Energy Fluences in Iron -Water Benchmark Configurations for the Verification of Monte Carlo Calculations and their Application in Reactor Material Dosimetry," *J. Nucl. Sci. Technol.*, vol. 39, no. sup2, pp. 947–950, 2002.

[4] S. Hübner, A. Knospe, M. Viebach, C. Lange, and A. Hurtado, "Experimental determination of the zero power transfer function of the AKR-2," *Physor 2020*, 2020.

[5] F. Vitullo, V. Lamirand, J.-B. Mosset, P. Frajtag, O. Pakari, G. Perret, and A. Pautz, "A mm 3 Fiber-Coupled Scintillator for In-Core Thermal Neutron Detection in CROCUS," *IEEE Trans. Nucl. Sci.*, vol. 67, no. 4, pp. 625–635, Apr. 2020.

[6] U. Kasemeyer, R. Früh, J. M. Paratte, and R. Chawla, "Benchmark on Kinetic Parameters in the CROCUS Reactor," in *International Reactor Physics Experiments Handbook (IRPhE)*, no. 4440, OECD, Ed. 2007, p. 94.

[7] L. Beyer, M. Fussan, and M. Krautz, "CT of detectors." 2018.

6 Appendices

6.1 AKR-2 reactor kinetic data and transfer function

Table 8: MCNP simulated precursor parameters [4]

Group of precursor	β_i	Std. dev.	λ_i in s^{-1}	Std. dev. in s^{-1}
1	0.00027	0.00001	0.01334	0.00001
2	0.00137	0.00002	0.03273	0.00001
3	0.00133	0.00002	0.12079	0.00001
4	0.00296	0.00003	0.30293	0.00001
5	0.00123	0.00002	0.85011	0.00001
6	0.00050	0.00001	2.85508	0.00003
Sum	0.00766	0.00004	-	-

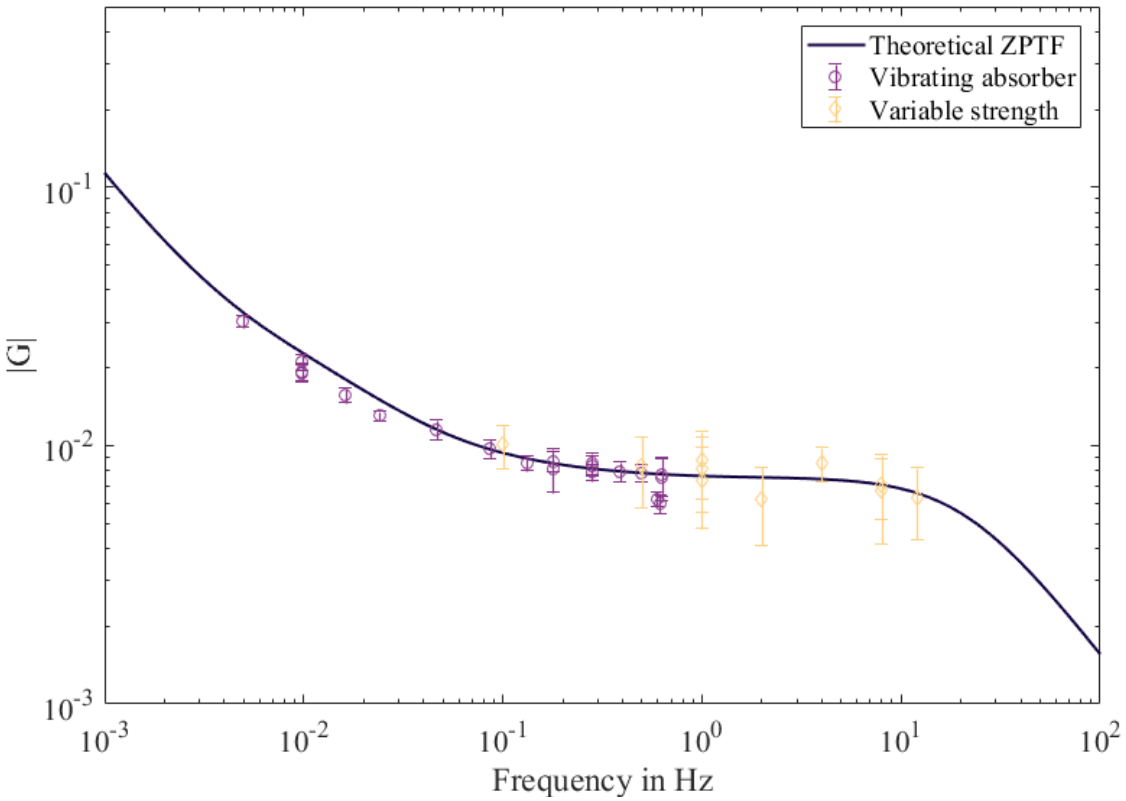

Figure 19: AKR-2 zero power transfer function, amplitude response [4]

6.2 Specifications of the detectors of the AKR-2 campaign

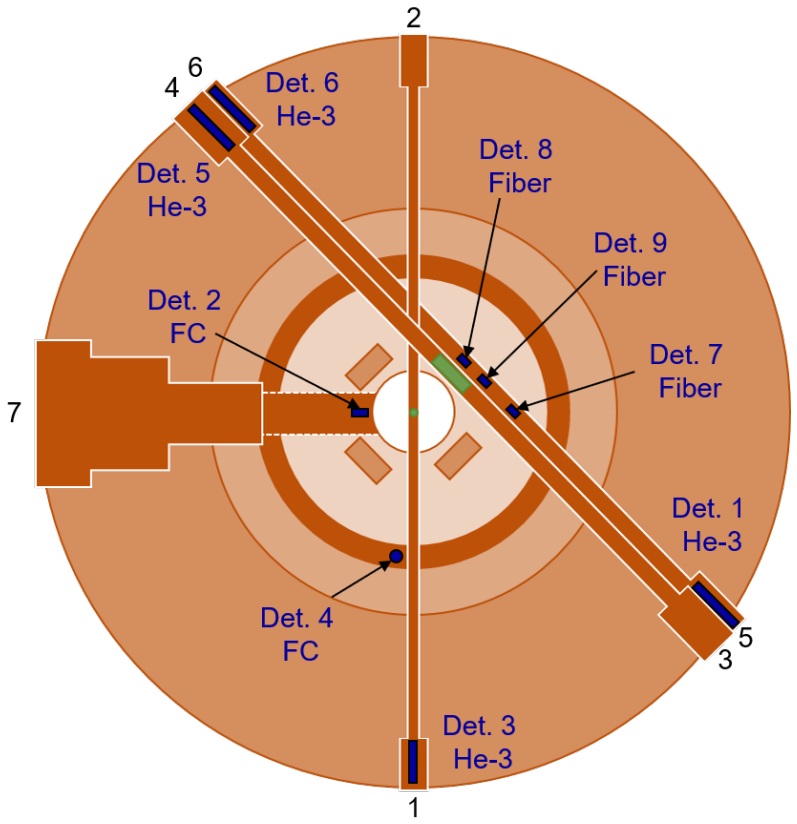

Figure 20: Positions of the detectors

6.2.1 Detector 1

Detector 1 is a Helium-3 counter and located at the entrance 5 of the lower tangential channel 5-6. It is the same detector at the same position as in campaign 1.

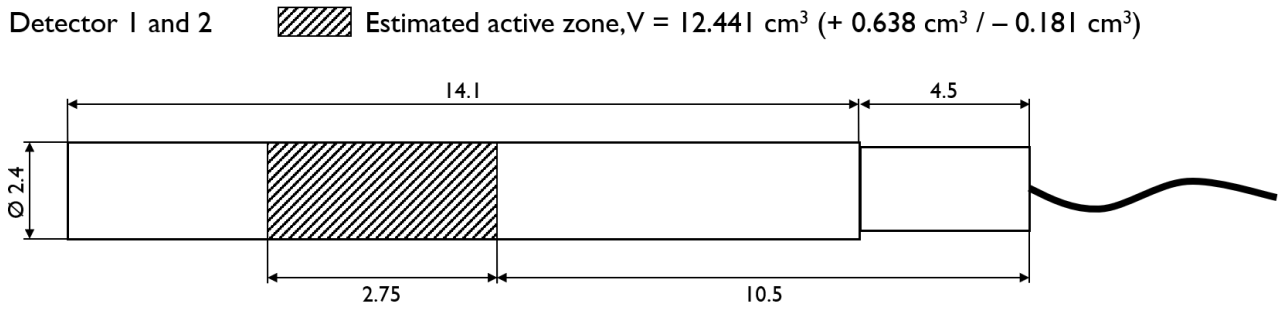

Figure 21: Dimension of the detectors 1 and 2 and their effective volume

The dimensions of the detector can be seen in Figure 21 as well as in the CT scan in Figure 22.

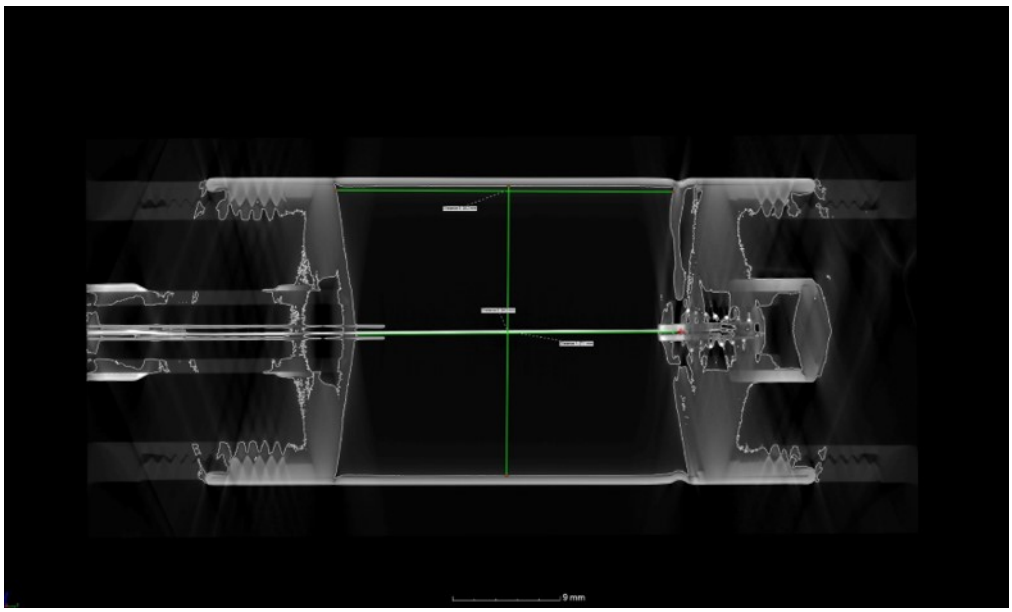

Figure 22: Micro CT of the detectors 1 and 2 [7]

6.2.2 Detector 2

Detector 2 is a relatively small fission chamber located as near as possible to the core in channel 7. It is run in pulse mode.

6.2.3 Detector *3*

Detector 3 is a Helium-3 counter. It is the first of three He-3 counters of a kind, used for this campaign. It is located at the outlet 1 of the small central channel 1-2.

6.2.4 Detector *4*

Detector 4 is a permanently installed fission chamber for the control of the reactor's operation. It is large compared to the other fission chamber (detector 2). As the Beagle-Bone (BB) acquisition system just could acquire one signal, this detector was just used for the absorber of variable strength (rotating device): for the linear motor axis operation, the BB was necessary to record the relative axis position.

6.2.5 Detectors 5 and 6

Detectors 5 and 6 are two He-3 counters of the kind and size of detector 3. They were located at the end of the channel 4, respectively 6.

6.2.6 Detectors 7, 8 and 9

Detectors 7, 8 and 9 are three miniature scintillators couple to optical fibers are located in the channel 5-6. With scintillator 2 (detector 8) at the centre of the channel, scintillator 3 (detector 9) 10 cm away from it and scintillator 1 (detector 7) 30 cm from the centre.
They were positioned with the help of an aluminium profile, where scintillator 1 was in the top groove, scintillator 2 in the groove nearer to the core centre and scintillator 3 in the groove opposite to the scintillator 2.

Table 9: Complete list of experiments

No	date	type	freq in Hz	center in cm axis	amp in cm	DwT in ms	1 MCS	2 FPGA	3 MCS	4 FPGA	5 FPGA	6 BB	7 FPGA	8 FPGA	9 EPFL	10 EPFL	11 EPFL	Pos rot (8 FPGA)	Pos Axis (BB)	Pos rot (Osci EPFL)
1	06.07.2020	AVS	2			40	x	no	x	no	x	x	x	x	x	x	x	?	no	no
2	07.07.2020	AVS	2			30	x	no	x	no	x	x	x	x	x	x	x	?	no	no
3	07.07.2020	AVS	0,1			30	x	no	x	no	x	x	x	x	x	x	x	?	no	no
4	07.07.2020	AVS	0,1			30	x	no	x	no	x	x	x	x	x	x	x	?	no	no
5	07.07.2020	AVS	4			30	x	no	x	no	x	x	x	x	x	x	x	?	no	no
6	07.07.2020	AVS	4			30	x	no	x	no	x	x	x	x	x	x	x	?	no	no
7	07.07.2020	AVS	1			30	x	no	x	no	x	x	no	x	x	x	x	?	no	no
8	08.07.2020	AVS	2			30	x	x	x	x	x	x	x	x	x	x	x	?	no	no
9	08.07.2020	VA	2	14,5	0,5	30	x	no	x	no	no	x	no	no	x	x	x	no	no	no
10	08.07.2020	VA	0,1	14,50	0,5	30	x	no	x	no	no	no	no	no	x	x	x	no	x	no
11	08.07.2020	VA	7	15	1	30	x	x	x	x	x	no	x	x	x	x	x	no	x	no
12	08.07.2020	VA	0,01	15	0,5	60	x	x	x	x	x	no	x	x	x	x	x	no	x	no
13	08.07.2020	VA	0,01	15	0,5	60	x	x	x	x	x	no	x	x	x	x	x	no	x	no
14	09.07.2020	AVS	2			40	x	x	x	x	x	no	x	x	x	x	x	?	no	no
15	09.07.2020	VA	0,01	10,5	2	60	x	x	x	x	x	no	x	x	x	x	x	no	x	no
16	09.07.2020	VA	0,01	10,5	2	60	x	x	x	x	x	no	x	x	x	x	x	no	x	no
17	09.07.2020	VA	1	10,5	2	30	x	x	x	x	x	no	x	x	x	x	x	no	x	no
18	09.07.2020	VA	1	10,5	2	30	x	x	x	x	x	no	x	x	x	x	x	no	x	no
19	09.07.2020	VA	4	16	3	30	x	x	x	x	x	no	x	x	x	x	x	no	x	no
20	09.07.2020	VA	2	16	3	30	x	x	x	x	x	no	x	x	x	x	x	no	x	no
21	10.07.2020	AVS	2			30	x	x	x	x	x	x	x	x	x	x	x	?	no	x
22	10.07.2020	VA	2	16	3	30	x	x	x	x	x	no	x	x	x	x	x	no	x	no
23	10.07.2020	both	2	14,5	0,5	30	x	x	x	x	x	no	x	x	x	x	x	?	x	x
24	10.07.2020	both	0,1	14,5	0,5	60	x	x	x	x	x	no	x	x	x	x	x	?	x	x
25	10.07.2020	VA	0,1	14,5	0,5	30	x	x	x	x	x	no	x	x	no	no	no	no	x	x
26	10.07.2020	both	2	16	3	30	x	x	x	x	x	no	no	x	x	x	x	?	x	x
27	10.07.2020	VA	0,1	14,5	0,5	30	x	x	x	x	x	no	x	x	x	x	x	no	x	no

6.3 Specifications of the detectors of the CROCUS campaign

6.3.1 Photonis CFUL01 fission chamber

The Photonis CFUL01 fission chamber consists in a large tube with a 1-g ^{235}U coating, the internals are described in Figure 23. During the experimental campaign, it was set first in a Faraday cage consisting in an aluminum tubing, and then inserted in a PMMA in-air experimental channel, all set vertically below the superior grid (see Figure 24).

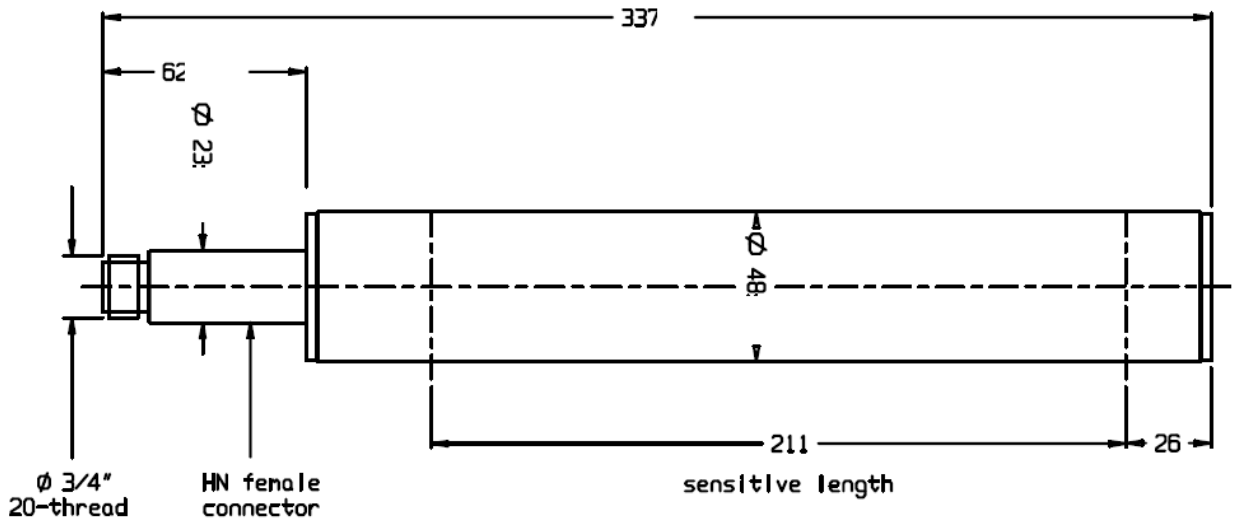

Figure 23 – Schematic of the Photonis CFUL01 fission chamber.

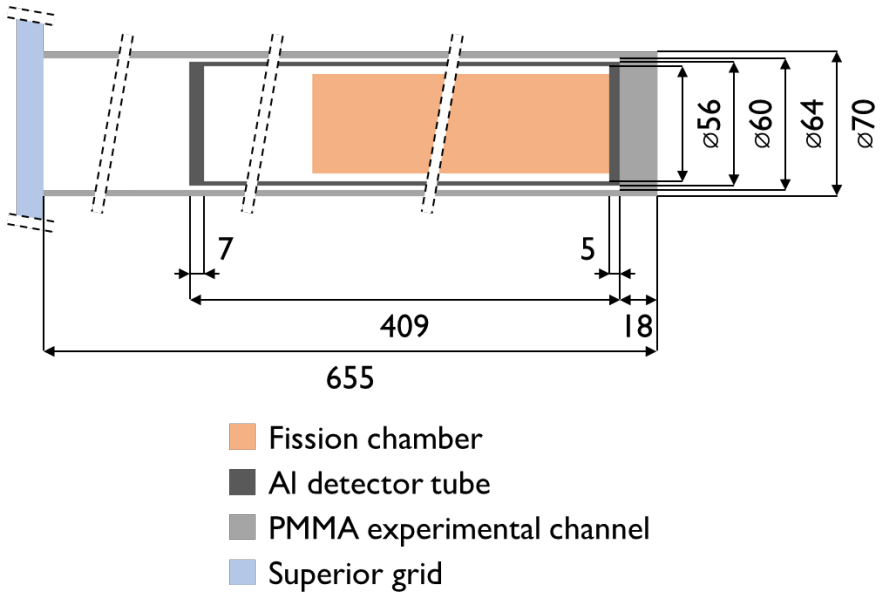

Figure 24 – Schematic of the fission chamber tube and in-air experimental channel with respect to the superior grid. NB: the channel is set vertically in-core, left side is top.

6.3.2 BF_3 proportional counters

Two types of BF_3 proportional counters were employed. Limited specification is available from the manufacturers for the Transcommerce International MN-1 detectors, and an x-ray image of the internals was carried out confirming them (see Figure 25). For the other and smaller BF_3 "grey" detectors, no information is available, neither series nor manufacturer. An x-ray image is considered, for now only the external dimensions are available. A summary of available information is presented in Table 10. The MN-1 PC were installed in in-air experimental channels lying at the bottom of the core, and whose diameter dimensions are presented in Figure 26. The others two "grey" detectors were set in the control rod guide tube (equivalent to an in-air U_{metal} cladding).

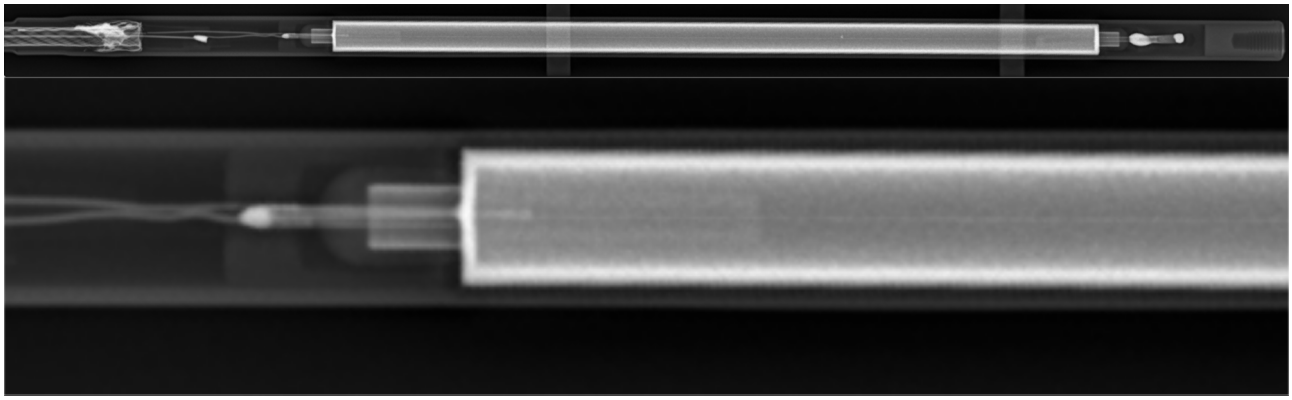

Figure 25 – X-ray image of a Transcommerce International MN-1 detector.

Table 10 – Specifications of the BF_3 proportional counters, from the supplier in the case of the Transcommerce International MN-1 detector, measured (casing) and estimated (active) for the "grey" smaller detector.

Supplier	Detector	Length (cm)			Diameter (cm)	
		Total	Al casing	Active	Al casing	Active
Trans. International	MN-1	25	18.4	12.7	0.75	0.63
Unknown	"Grey"	-	14.1	est. ~8.4	0.75	est.~0.63

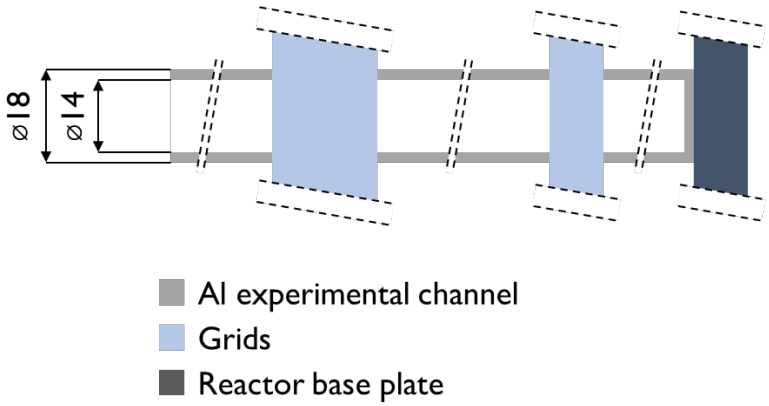

Figure 26 – Schematic of the in-air aluminum experimental channel used by the MN-1 BF_3 proportional counters, with respect to the grids and the reactor base plate. NB: the channel is set vertically in-core, left side is top.

6.3.3 *^{3}He proportional counters in Polyethylene and Cd sheats*

The ^{3}He detectors were set in a sheath of polyethylene and cadmium in order to cut their sensitivity to thermal neutrons (Cd), and enhance their sensitivity to fast neutrons (PE). All dimensions are indicated in Figure 27.

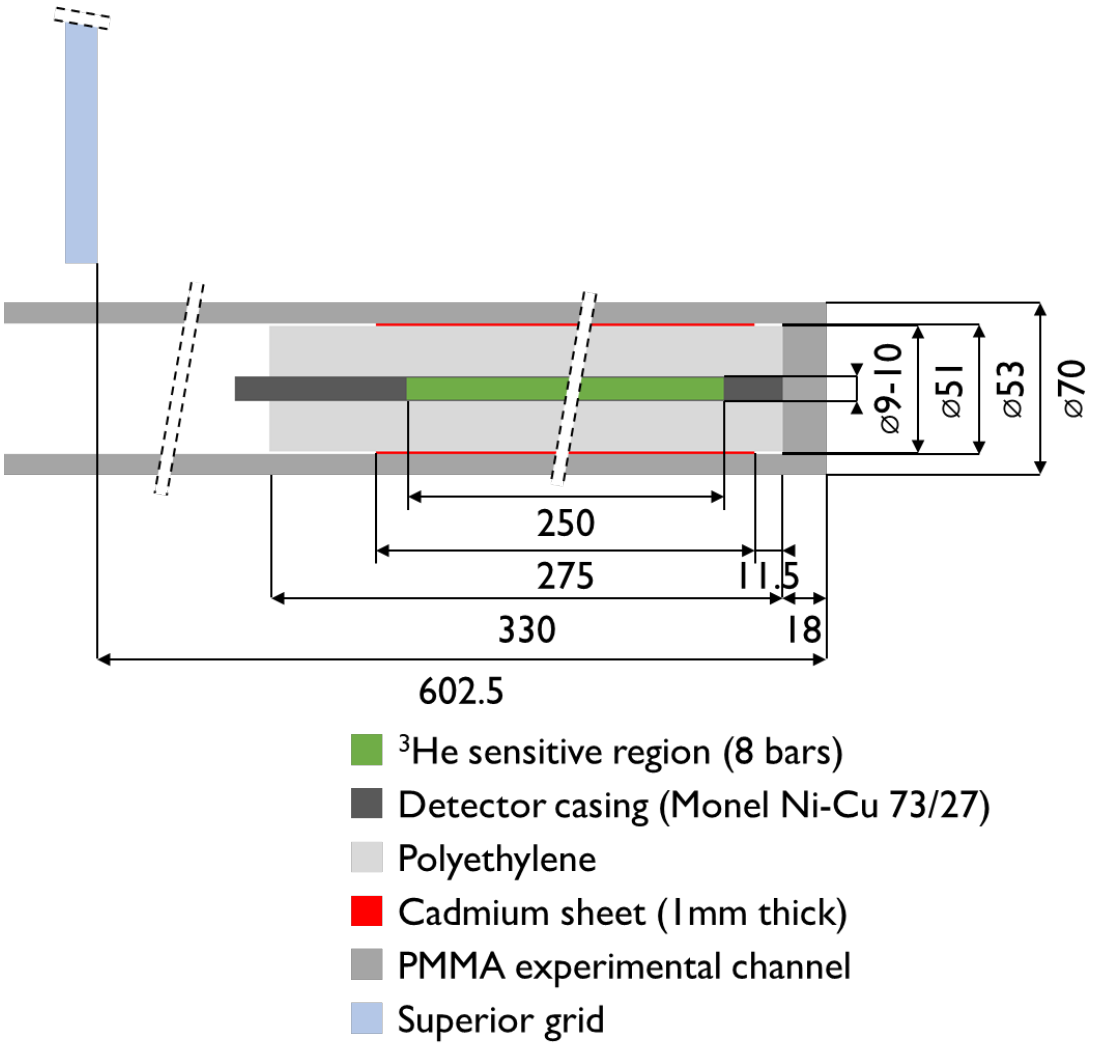

Figure 27 – Schematic of an ^{3}He detector set in its in-air experimental channel.

Table 11 – Specifications of the He-3

Supplier	Model	Length (cm)		Diameter (cm)	
		Total	Active	Total	Active
Canberra	12NH25/1F	34,4	250	1.0	0.9

6.3.4 *Photonis CFUF34 miniature fission chamber (TRAX)*

The Photonis CFUF34 1-mg ^{235}U-coated miniature fission chamber is part of the CROCUS reactor system called TRAX. It allows translating radially and axially this watertight miniature detector along the slit between the two superior half-grids. It was set at core center during the whole measurement campaign.

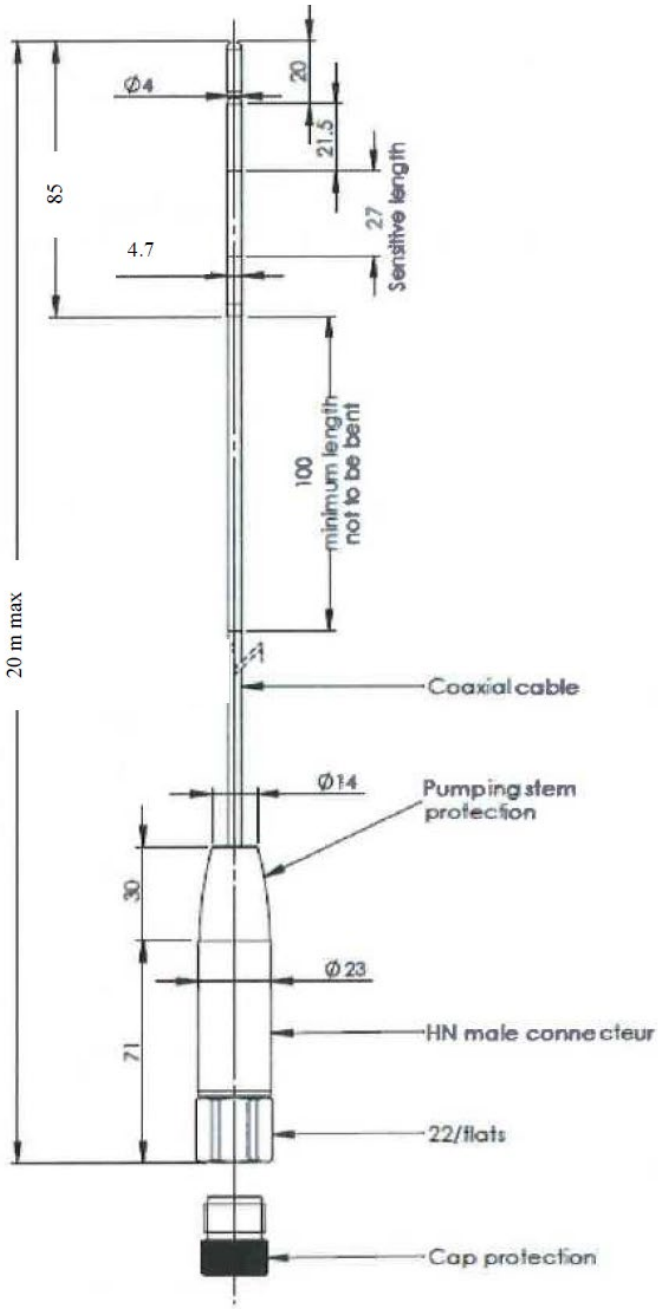

Figure 28 – Schematic of the Photonis CFUF34 miniature fission chamber. NB: the detector's side is at the bottom when set in-core.